JCEEA

Czasopismo Inżynierii Lądowej, Środowiska i Architektury

Journal of Civil Engineering, Environment and Architecture

Kwartalnik
tom XXXVI
zeszyt 66 (nr 3/2019)
lipiec-wrzesień

(e-ISSN 2300-8903)

Czasopismo Inżynierii Lądowej, Środowiska i Architektury jest kontynuacją
Zeszytów Naukowych Politechniki Rzeszowskiej - Budownictwo i Inżynieria Środowiska.

Issued with the consent of the Rector

Editor in Chief Publishing House of Rzeszow University of Technology
Professor Grzegorz OSTASZ, DSc, PhD

e-ISSN 2300-8903; p-ISSN 2300-5130

The electronic version of the Journal is an original version

Editorial Office: Rzeszow University of Technology, Faculty of Civil and Environmental Engineering and Architecture, St. Poznańska, 35-084 Rzeszów, Poland, www.oficyna.prz.edu.pl//pl/zeszyty-naukowe/czasopismo-inzynierii-ladowej-s/ (e-mail: jceea_bud@prz.edu.pl)

Publisher: Publishing House of Rzeszow University of Technology, 12 Powstanców Warszawy Ave., 35-959 Rzeszow, www.oficyna.prz.edu.pl (e-mail: oficyna@prz.edu.pl)

Additional information and an imprint – p. 77

Table of Contents

Grażyna SAKSON, Agnieszka BRZEZIŃSKA, Krzysztof KOWALSKI:
Monitoring, Early Warning And Sustainable Management System
for Lodz Wastewater Treatment Plant as a Water Protection Tool 5

Dorota SZAL, Renata GRUCA-ROKOSZ: Heavy Metal Contamination
in Sediments of Rzeszów Reservoir (Poland) 17

Marcin KACZMARZYK, Aleksander WAŚNIOWSKI: Internal Heat Loads
in Lunares Analogue Planetary Base – a Case Study 25

Jakub ŻYWIEC: Using the Weibull ++ Software in Water Supply Network
Failure Analysis 37

Rafał BUDZIŃSKI: Numerical Analysis of Cable Net Structure
with Application of Different Pretensioning Methods 47

Maciej PIEKARSKI: Renewal of Selected Fragments of Rzeszów Based
on the Lost Symbols and Functions of Places as a Means
of Strengthening the City's Identity 65

CZASOPISMO INŻYNIERII LĄDOWEJ, ŚRODOWISKA I ARCHITEKTURY
JOURNAL OF CIVIL ENGINEERING, ENVIRONMENT AND ARCHITECTURE
JCEEA, t. XXXVI, z. 66 (3/19), lipiec-wrzesień 2019, s. 5-16, DOI:10.7862/rb.2019.13

Grażyna SAKSON[1]
Agnieszka BRZEZIŃSKA[2]
Krzysztof KOWALSKI[3]

MONITORING, EARLY WARNING AND SUSTAINABLE MANAGEMENT SYSTEM FOR LODZ WASTEWATER TREATMENT PLANT AS A WATER PROTECTION TOOL

Municipal wastewater treatment plants are exposed to the inflow of toxic substances, which may hamper or even preclude their proper functioning, especially of the biological part. In the case of combined or hybrid sewer systems, additionally, in wet weather, there may appear a rapid inflow of a mixture of domestic and industrial sewage, and stormwater in an amount exceeding the capacity of the devices, causing the need to discharge parts of not fully treated wastewater through the bypass channel, which may reduce overall treatment effects. In such situations, the receivers are exposed to an inflow of increased amounts of pollutants, which on the one hand causes a threat to the aquatic environment, on the other, may result in administrative fines for the treatment plant resulting from non-compliance with the conditions of the water permit, as well as costs of removing the effects of failure. The article presents the concept of a monitoring, early warning and sustainable management system for the Lodz wastewater treatment plant, which will allow minimizing pollutant emissions to the aquatic environment. The system will be based on data from the municipal pluviometer network, measurement of flows in combines sewer overflows and newly built sewage quality monitoring stations equipped with on-line probes. The resulting data will allow to predict quantity and quality of inflow to the treatment plant, which will allow for an early warning about the dangers. In consequence decision-making to improve the safety of its operation will be possible.

Keywords: sewer system, sewage treatment, water protection, predictive model, toxicity

[1] Corresponding author: Grażyna Sakson; Lodz University of Technology Institute of Environmental Engineering and Building Installations, Al. Politechniki 6, 90-924 Łódź; grazyna.sakson-sysiak@p.lodz.pl. http://orcid.org/0000-0002-6022-7771

[2] Agnieszka Brzezińska; as above; agnieszka.brzezinska@p.lodz.pl; http://orcid.org/0000-0001-5913-8029

[3] Krzysztof Kowalski; Wastewater Treatment Plant of Lodz, Ltd. Sanitariuszek 66, 93-469 Łódź; krzysztof_kowalski@gos.lodz.pl

1. Introduction

Municipal wastewater treatment plants (WWTP), due to the increasing requirements of environmental protection, have to meet more and more stringent requirements regarding both the quality of discharged sewage and operational reliability. This is sometimes difficult due to unforeseen situations, usually independent of the sewer network operator and sewage treatment plant. Municipal WWTPs are exposed not only to technical equipment failures, but also to an uncontrolled inflow of toxic substances that can inhibit biological treatment processes and, in extreme cases, lead to their breakdown. Such situations may be caused by intentional action (illegal discharge of wastewater into the sewage system), but also may be the effect of introduction of new substances and products, which in turn results in the introduction of new contaminants to a treatment plant, whose effects on living organisms is not fully recognized. In the case of combined sewage system, hydraulic overload resulting from stormwater inflow after prolonged and intense rainfall, is an additional threat, which may also worsen the effects of treatment. In both cases, not fully treated wastewater may be discharged to the receiver. Such situation causes a threat to the aquatic environment on the one hand, and on the other may result in financial penalties for treatment plants, resulting from non-compliance with the conditions for sewage disposal, as well as costs of removing the effects of failure (e.g. restoration population of microorganisms in activated sludge chambers).

According to the current legal status in Poland, the requirements for the quality of sewage discharged to the receiver increase with the size of the treatment plant, but they do not take into account the size and absorbency of the receiver, which is crucial for the possibility of maintaining its good condition or good ecological and chemical potential. The impact of discharged wastewater on the receiver depends primarily on the pollutant load and the dynamics of emissions, and of course depends on the size of the receiver. Rapid changes in the level of pollutant emissions are dangerous especially for small receivers, which is why sewage treatment plants discharging sewage to them should be particularly well protected against the possibility of discharge of not fully treated sewage.

Significant sudden changes in the quality of inflow to WWTP, and primarily the presence of toxic substances, can affect the reduction of the biological treatment efficiency. In particular, nitrifying bacteria are sensitive to the effects of toxic factors such as increased heavy metal concentration, pH changes, reduced oxygen concentration and rapid changes in ammonium nitrogen concentration in the inflowing sewage [1]. Wastewater toxicity is more and more often the subject of research, however, generally used methods do not allow its simple and reliable on-line measurement. Attempts to establish a correlation between sewage toxicity and physicochemical parameters are not effective yet. Vasquez and Fatta-Kassinos [2] have only established that two parameters: conductivity and ammonium nitrogen concentration are related to toxicity. Research conducted by Liwarska-

Bizukojć et al. [3] in the wastewater treatment plant in Zgierz did not show any significant correlation between toxicity and basic parameters of wastewater (pH, BZT_5, COD, ammonium nitrogen, total nitrogen, total phosphorus), and their biodegradability BZT_5/COD). Only a weak correlation was found between the conductivity and toxicity of raw wastewater in the short-time summer campaign.

Rapid changes of inflow may cause difficulties in optimal control of municipal sewage treatment plants cooperating with the combined sewer system which is largely due to the unpredictability of precipitation. For this reason, attempts to forecast inflow to the treatment plant with sufficient time in advance are being made in the world. Based on rainfall data (currently occurring or forecast from radar data) and measurements of sewage depth and flow in the sewers, RTC (Real Time Control) systems are being created {4, 5]. Solutions for forecasting the WWTP inflow using artificial intelligence methods, such as neural networks, neural-fuzzy networks, etc. are also being developed [6-8]. Attempts to include into these systems tools that enable qualitative forecasting of inflows are being made [9]. According to Vezzaro et al. [8] controlling the sewage system based on the measurement of WWTP inflow quality allows to mitigate the effects of first wave of pollutants phenomenon.

However, there are currently no solutions enabling comprehensive forecasting of both the sewage inflow to the treatment plant and the concentration and loads of pollutants. Meanwhile, early warning of treatment plants about the possibility of hazards could enable, for example, storage of some wastewater not only to avoid hydraulic overloads, but also inflow of toxic substances or excessive loads of pollution to the biological part. This would create a chance for optimal control of treatment processes in all conditions and, as a consequence, better protection of the sewage receiver. Such a system is currently being developed in Lodz as part of the project “Development of a monitoring, early warning and sustainable management system for wastewater treatment plants minimizing emissions to the aquatic environment from the urbanized area” implemented by the scientific and industrial consortium: Lodz University of Technology and Wastewater Treatment Plant of Lodz, Ltd.

2. Characteristics of Lodz sewer system and WWTP

Lodz is equipped with a hybrid sewage system. In the central part there is a combined sewer system with 4 main collectors running from the north-east to the south-west of the city towards the Group Wastewater Treatment Plant of the Lodz Agglomeration (GOŚ ŁAM). Two sanitary sewers collecting sewage from northern and south-eastern regions of Lodz are included in this system. Two sewage collectors from Pabianice and Konstantynów Łódzki are connected to the system prior to WWTP. There are 18 combined sewer overflows in the combined sewerage in Lodz, equipped with a flow measurement system.

Currently, wastewater from the cities of Łódź, Pabianice, Konstantynów Łódzki and the municipalities of Nowosolna and Ksawerów flows into GOŚ ŁAM. These areas are inhabited by nearly 800 thousand people. The designed capacity of the treatment plant is 1.026.260 PE**,** while the actual load on the treatment plant, calculated on the basis of operational data from 2015-2017, is currently 934.700 PE. Maximum sewage inflow to the treatment plant during wet weather for a probability of 85% is 166,000 m^3 per day.

Wastewater flowing into the wastewater treatment plant is first subjected to mechanical treatment in the screens building, than wastewater flows into the grit chamber. The final facilities of mechanical wastewater treatment are rectangular preliminary settling tanks. Biological sewage treatment is carried out in activated sludge chambers operating in MUCT technology. The following zones are separated in each technological line:

- anaerobic compartment,
- anoxic compartment,
- aerobic compartment.

The final treatment facilities are rectangular secondary settling tanks blocked with activated sludge chambers. The separated sludge is discharged to four recirculation pumping stations, where its main stream is directed back to the activated sludge chambers, and some removed as excess sludge for further processing in the sludge treatment plant part. The treatment plant scheme is presented in Fig. 1.

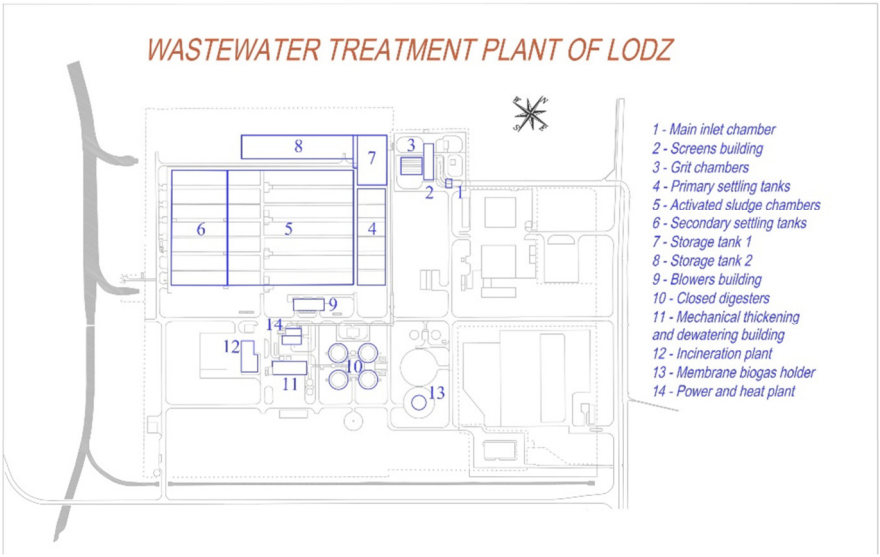

Fig. 1. Schematic of the Group Wastewater Treatment Plant of the Lodz Municipal Agglomeration

In dry weather, the sewage inflow to the treatment plant, in terms of both quantity and quality, is stable. Under these conditions, the characteristics of the inflow during the day or week are repeatable, and its changes are relatively small. It is different during wet weather, when the amount of inflowing sewage increases significantly, sometimes rapidly, and can cause WWTP overload, especially the biological part. Therefore, there are situations in which not all wastewater flowing into the GOŚ ŁAM is fully treated. Part of the wastewater after the primary settling tanks, and in extreme cases after the grit chambers, is directed to the bypass channel, which may contribute to increased emission of pollutants to the receiver compared to other periods.

Although in recent years the annual rainfall in the city and the number of wet weather days do not show an upward trend, the occurring rainfall is characterized by a higher maximum intensity, which may cause a rapid increase in the sewage inflow to the treatment plant (Fig. 2).

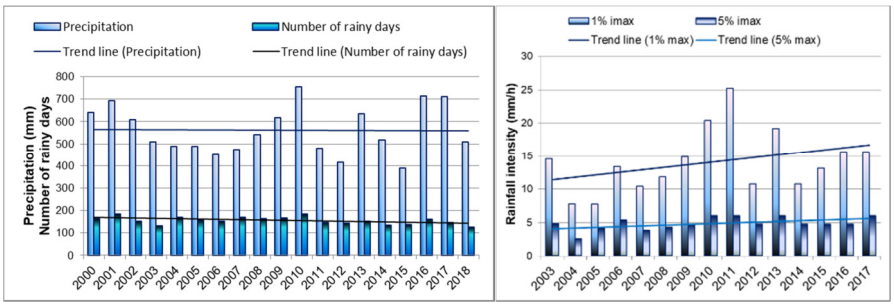

Fig. 2. Precipitation height and number of days with precipitation (a) and the intensity of precipitation with the highest intensity (mm/h) according to 5-minute records (data for 1% and 5% of highest values and trend lines) (b)

Measurements of sewage inflow to GOŚ ŁAM indicate that for about half the days in a year the sewage treatment plant has to cope with increased inflows resulting from precipitation, and several or more times a year the volume of inflowing sewage exceeds twice the reliable maximum flow for the sewage treatment plant, which releases from the need to meet requirements contained in the water-legal permit regarding the composition of discharged wastewater (Table 1). In such cases, some of the wastewater is discharged through a bypass channel without biological treatment. Storage them could help avoid such situations.

Table 1. Number of exceedances of the daily sewage inflow to GOŚ ŁAM Qd in relation to the maximum dry weather flow for WWTP Q_m =166.000 m^3/day

Year	$Qm<Q_d<2Q_m$		$Q_d>2Q_m$	
	monthly	per year	monthly	per year
2017	4-29	201	0-4	14
2018	1-25	143	0-2	5

The analyzes carried out using the US EPA SWMM program have shown that an effective solution limiting sewage discharge to bypass channel is the construction of storage tanks {10,11]. The effectiveness of such tanks depending on their volume is shown in Fig. 3.

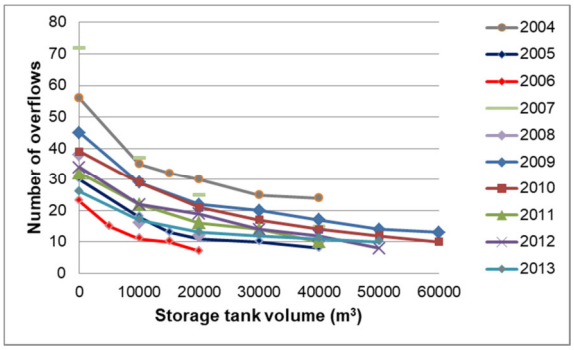

Fig. 3. Impact of separated storage tank volume on the reduction of biologically untreated sewage discharge by the bypass channel at GOŚ ŁAM [11]

It is also possible to use in-sewer storage in the main sewer Polesie XV prior the WWTP with the RTC system. The detention would be forced by 4 pairs of gates installed in the sewer. Exemplary effects of such a solution are presented in Fig. 4.

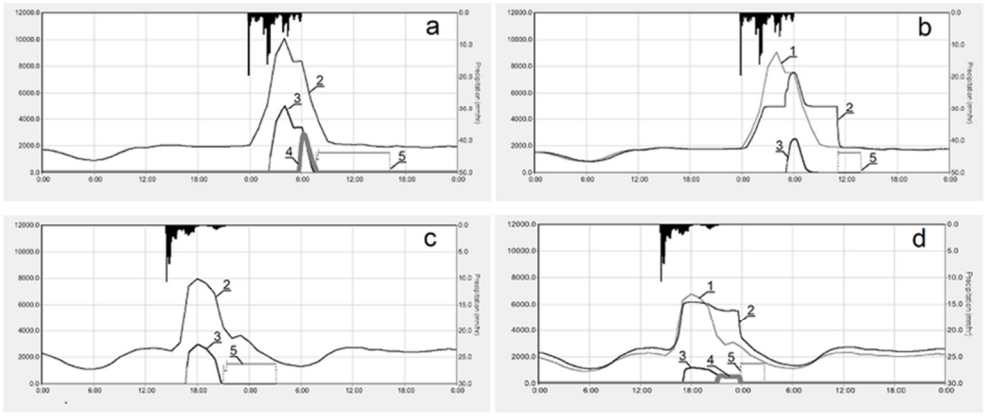

Fig. 4. Example of simulation of WWTP operation with the storage tanks, flow (l/s):
a, b - example of a rainfall with overflow in case of sewage storage in tanks (a) and without overflow in case of additional storage in Polesie XV (b); c, d - example of a rainfall without overflow in case of sewage storage in tanks (c); and with overflow in case of additional storage in Polesie XV (d);
1–inflow to main sewer Polesie XV; 2–inflow to WWTP; 3–inflow to storage tank; 4–overflow from storage tank; 5–storage tank emptying; right axis – precipitation (mm/hr)

Quality of wastewater flowing into WWTP may also change significantly during the wet weather. Strormwater, which in this period may constitute the majority of the entire inflow volume (depending on precipitation parameters) may carry a significant amount of pollutants washed out from the catchment and leached from the sewer deposits, hindering the treatment process. In wet weather, as well as during snowmelt, inflows to WWTP are often characterized by the occurrence of the first flush phenomena. This means that in the beginning of precipitation may in the mixture of municipal wastewater and stormwater much larger amount of pollutants may flows to WWTP than in the further runoff.

The inflow of a large amount of pollutants in very short time, even if there are no toxic substances among them, can cause significant difficulties in the treatment process. Changes in the quality and quantity of sewage flowing into WWTP are not repeatable, they depend primarily on rainfall characteristic and the length of the dry weather period before precipitation, which determines the amount of pollution built-up on the catchment and wash-off during rainfall. Even on the same catchment, in the case of different precipitation, the first flush phenomenon may not be observed, it may be pronounced or the so-called the last wave phenomenon may occur, moreover, the flow of pollutants may be different for basic quality parameters of sewage (Fig. 5).

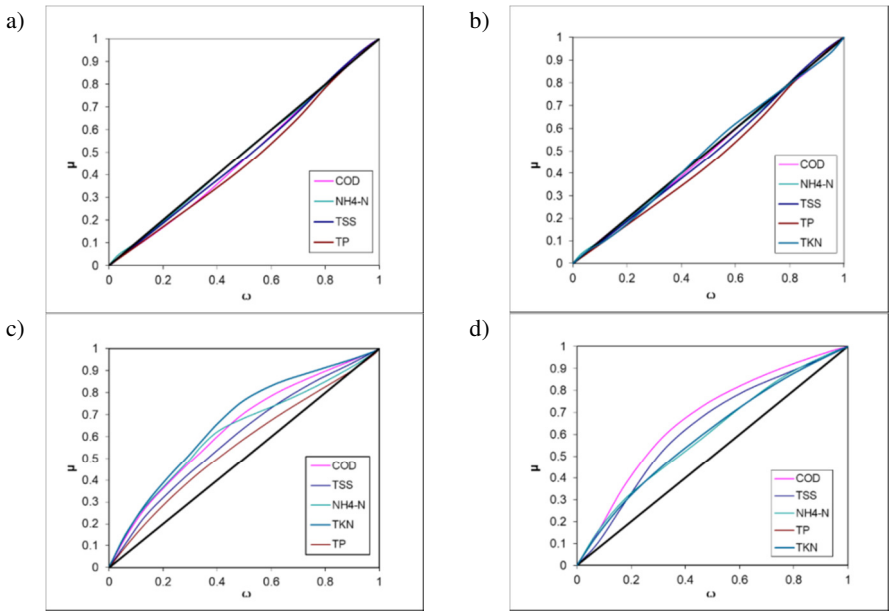

Fig. 5. Analysis of the first flush phenomena in inflow to GOŚ ŁAM: a) storm with a high intensity of precipitation; b) long rainfall of low intensity; c) long-lasting heavy rainfall; d) snowmelt combined with rainfall;
COD – chemical oxygen demand; TSS – total suspended solids; NH_4-N - ammonium nitrogen; TKN - total Kjeldahl nitrogen; TP - total phosphorus; ω - cumulative wastewater volume; μ - cumulative load

An important threat to the WWTP is the inflow of toxic substances that can cause inhibition of biological treatment processes. Such situations took place in September 2011 and April 2019, when as a result of the inflow of unidentified substances to GOŚ ŁAM, inhibition of the nitrification process was found, which resulted in limiting the reduction of nitrogen concentration, a significant increase in the emission of nutrients to the environment, and the threat of non-compliance with legal requirements. The process collapse was associated with the destruction of the nitrifying bacterial population, which is most sensitive to the effects of toxic agents. Restoration of the relevant nitrification process parameters is possible after the termination of toxic substances inflow, and taking action to accelerate the recovery of the bacterial population. This can be done by inoculating the activated sludge with sludge from other treatment plants and dosing preparations containing nitrifying bacteria. Regardless of chosen solutions, the reconstruction can take up to several weeks. This time depends on many factors, including the parameters of treatment process and the nitrogen load in sewage inflowing to WWTP.

As part of the Project "Sewage management, phase III in Łódź" implemented from the Cohesion Fund "The Operational Program Infrastructure and Environment 2014-2020, Priority II Environmental protection, including adaptation to climate change", two storage tanks for sewage flowing into the treatment plant are being built in GOŚ ŁAM:

- tank I (2-chamber) with a total volume of approx. 15,000 m^3;
- tank II (4-chamber) with a total volume of approx. 25,000 m^3.

Tanks volume was determined on the basis of many years of observation of inflows to the treatment plant and computer simulations [10]. The total useful capacity of the tanks (40,000 m^3) is to ensure the capture of most of the runoff after low and medium rainfall and the most polluted first flush of large runoff, exceeding the volume of the tanks.

Filling of tank I is foreseen after preliminary settling tanks - from the distribution channel to activated sludge chambers (ASC) or after grit chambers(GC), from the distribution channel to preliminary settling tanks (PST), through the designed channel valve. Filling of tank II will take place in a cascade system - after filling tank I or directly with sewage after PSP, from the distribution channel to ASC. The maximum sewage inflow to the preliminary settling tanks was assumed to be about 30,000 m^3 /h (above this inflow the excess sewage will be directed to tank I). It was assumed that the sewage inflow to ASC will not exceed the value of 18,200 m^3/h. Excess wastewater after PST, in the amount of approx. 12,000 m^3/h, will be directed through channel valves designed in the distribution channel on the ASC to the storage tank I. The tank chambers will be filled in cascade. After filling the first chambers, excess sewage will overflow to the common channel between tanks I and II, and then to tank II or to the bypass channel. Tank I will be emptied into PST distribution channel, while wastewater from tank II will be directed to distribution channel to ASC through a system of designed pump systems.

3. Concept of the system

Optimal use of storage tanks requires information on quality and quantity of wastewater flowing into the GOŚ ŁAM and the forecast of their changes. If the excess volume of wastewater after rainfall is taken over by the tanks, it will be possible to fully clean it after the increased inflow stops. Also, if significant changes in sewage quality are identified that may affect their biological treatment, it will be possible to divert this type of inflow to tanks. Therefore, having information on the current composition of sewage in the sewer system and forecasting inflow to the treatment plant will facilitate optimal use of the technological possibilities of WWTP. The above premises, analysis of the current state of knowledge and technical capabilities, as well as experience in the field of monitoring and modelling of the Lodz sewage system constitute the basis for the development by Lodz University of Technology, Institute of Environmental Engineering and Building Installations, and Wastewater Treatment Plant of Lodz, Ltd. the prototype of monitoring, early warning and sustainable management system for GOS ŁAM.The system will be based on measurement data from three main sources, these are:

- existing pluviometer system in the city, consisting of 18 raingauges, of which 5 are located on the combined catchment,
- flow measurement system in sewers next to 18 combined sewer overflows,
- newly constructed 4 stations (Fig. 6) for qualitative monitoring of wastewater in the sewage system with on-line sensors measuring min. 8 parameters on each station (pH, conductivity, organic substances, ammonium nitrogen, suspended solids/turbidity, chlorides, BTX, hydrogen sulphide). Research on sewage quality with on-line probes conducted on the J1 CSO since 2011, as well as previous tests on the inflow to GOŚ ŁAM [12] showed that these types of stations can be successfully used for assessment of sewage quality and amount of pollutant emissions from the sewage system.

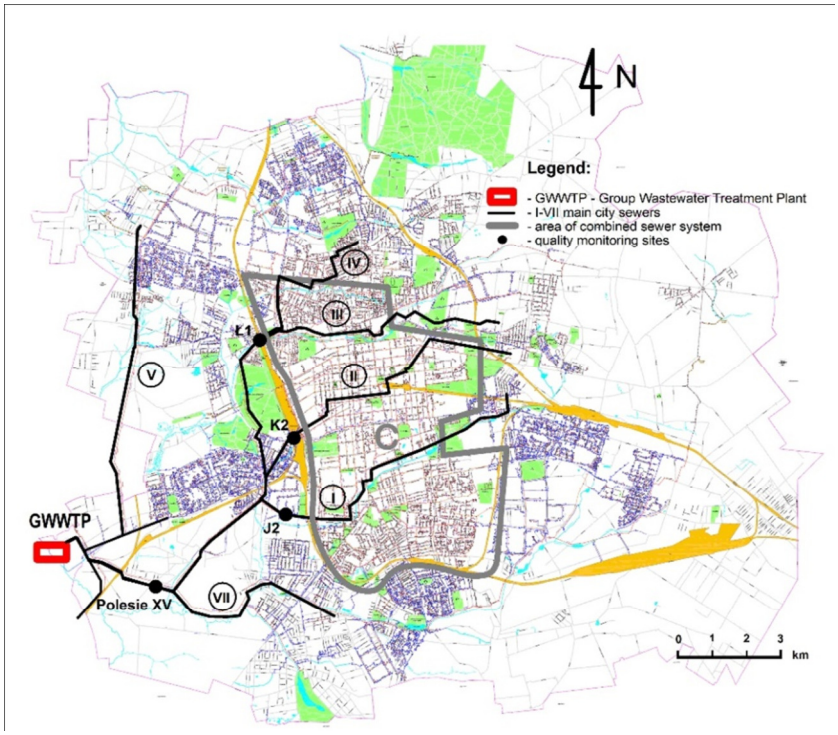

Fig. 6. Location of sewage quality monitoring stations in the Lodz sewage system

The benefits of introducing the system include:

- receiving, well in advance, reliable information by sewage treatment plant employees on anticipated significant quantitative and qualitative changes in inflowing sewage and the possibility of a threat to biological treatment processes. This creates the opportunity to optimally control the treatment plant, both the parameters of the treatment process and flows;
- ability to direct part of the wastewater into storage tanks (especially after receiving information about the potential toxicity), or - in exceptional cases - to a bypass channel. In a situation where there is a suspicion of the inflow of hazardous substances, the tanks will allow for their storage, collection of sewage samples and their analysis as well as determination of the way to proceed (referring to biological treatment or neutralization);
- improving the quality of wastewater discharged to the receiving water in wet weather. The inflow of significant amounts of stormwater sometimes causing the necessity of discharging part of it through a bypass channel before biological treatment, as a result worsens the quality of sewage discharged by the treatment plant. According to the conducted analyses [13], limiting the operation of the bypass channel and the volume of discharges by 70% will allow reducing the emissions of basic pollutants by approx. 2.7–6.8%

depending on the parameter (BOD_5, COD, total suspended solids, total nitrogen and total phosphorus);
- avoiding unforeseen costs associated with the emission of sewage not meeting the quality requirements and the elimination of breakdowns.

The developed system will also enable visualization, archiving and reporting of data that can be used for further analyzes related to the modernization or expansion of the facility and its adaptation to climate change, urbanization and the growing requirements of receiving water protection.

The system, based on only 4 stations for monitoring the quality of sewage, will not yet allow full control of the inflow to the GOŚ ŁAM due to the existing sewer system layout in the city. Current research on sewage quality (including toxicity) in the entire sewer system should allow to determine the quality characteristics of sewage discharged from the whole catchment, which will allow more accurate inflow forecasting, but this will not take into account uncontrolled pollutant discharges into not monitored sewers. For this reason, the system will probably need to be expanded in the future. The developed system should be characterized by reliability in case of failure of one or more measuring elements - raingauges, flow meters or sensors used to sewage quality monitoring. The use of quantitative and qualitative on-line monitoring of the sewage system is a very convenient and promising tool that facilitates solving many operational and modernization problems, however it creates many operational difficulties. There may be gaps in measurements or the measurement data is of poor quality. However, it can be assumed that the rapid progress in the development of on-line measurement methods and the expansion of experience in the field of operation of this type of equipment will contribute to the improvement of the efficiency and reliability of such solutions.

4. Summary

The monitoring, early warning and sustainable management system currently being developed in Lodz will be an important technological innovation in the sewage disposal and treatment system enabling progress towards its fully balanced operation and will allow better protection of the receiving water. The construction of the system will enable the integration of the existing monitoring systems in the city with new elements, resulting in the creation of a modern, intelligent tool for environmental protection and optimization of expenses for this purpose.

"Project co-financed by the European Union financed from the European Regional Development Fund under the Smart Growth Operational Programme. The project is implemented as a part of the National Centre for Research and Development: Regional Science and Research Agendas competition."

References

[1] Black G., Jones M., Vale P., Johnson N., Nocker A., Cartmell E., Dotro, G., Biofilm Responses to Toxic Shocks in Closed Pipes: Using Nitrous Oxide Emissions as an Early Warning of Toxicity Ahead of a Wastewater Treatment Works, Water, Air and Soil Pollution, 2014, 225, 2, 1837.

[2] Vasquez M.I., Fatta-Kassinos D., Is the evaluation of "traditional" physicochemical parameters sufficient to explain the potential toxicity of the treated wastewater at sewage treatment plants? Environ Sci Pollut Res, 2013, 20:3516–3528.

[3] Liwarska-Bizukojć E., Ślęzak R., Klink M., Study on wastewater toxicity using ToxTrak™ method, Environmental Science and Pollution Research, 2016, 23:9105–9113.

[4] García L., Barreiro-Gomez J., Escobar E., Téllez D., Quijanoa N., Ocampo-Martinez C., Modeling and real-time control of urban drainage systems: A review, Advances in Water Resources, 2015, 85, 120–132.

[5] Schilling W., Andersson B., Nyberg U., Aspegren H., Rauch W., Harremoës P., Real time control of wastewater systems, Journal of Hydraulic Research, 2010,785-797.

[6] Seggelke K., Löwe R., Beeneken T., Fuchs L., Implementation of an integrated real-time control system of sewer system and waste water treatment plant in the city of Wlhelmshaven, Urban Water Journal, 2013,10, 5, 330-341.

[7] van Daal P., Gruber G., Langeveld J., Muschalla D., Clemens F., Performance evaluation of real time control in urban wastewater systems in practice: Review and perspective, Environmental Modelling & Software, 2017, 95, 90-101.

[8] Vezzaro L., Christensen M.L., Thirsingd C., Grumb M., Mikkelsen P.S., Water quality-based real time control of integrated urban drainage systems: a preliminary study from Copenhagen, Denmark, Procedia Engineering, 2014,70, 1707–1716.

[9] Langeveld J., Van Daal P., Schilperoort R., Nopens I., Flameling T., Weijers S., Empirical sewer water quality model for generating influent data for WWTP Modelling, Water, 2017, 9, 491.

[10] Zawilski M., Sakson G., Analiza możliwości retencjonowania ścieków ogólnospławnych dla potrzeb Grupowej Oczyszczalni Ścieków w Łodzi, Katedra Inżynierii Środowiska PŁ na zlecenie GOŚ ŁAM, 2008.

[11] Sakson G., Zawilski M., Brzezinska A., Analysis of combined sewer flow storage scenarios prior to wastewater treatment plant, Ecological Chemistry and Engineering S, 2018, 25(4), 619–630.

[12] Brzezinska A., Zawilski M., Sakson G., Assessment of pollutant load emission from combined sewer overflows based on the online monitoring, Environmental Monitoring and Assessment, 2016, 188, 9.

[13] Zawilski M., Sakson G., Brzezińska A., Zrównoważone gospodarowanie wodami opadowymi na obszarach zurbanizowanych w aspekcie ochrony wód odbiornika, „Infrastruktura miast" pod red. J. Dziopaka, D. Słysia i A. Stec, Oficyna Wydawnicza Politechniki Rzeszowskiej, ISBN 978-83-7934-166-5, 2017.

Przesłano do redakcji: 22.08.2019 r.

CZASOPISMO INŻYNIERII LĄDOWEJ, ŚRODOWISKA I ARCHITEKTURY
JOURNAL OF CIVIL ENGINEERING, ENVIRONMENT AND ARCHITECTURE
JCEEA, t. XXXVI, z. 66 (3/19), lipiec-wrzesień 2019, s. 17-24, DOI:10.7862/rb.2019.14

Dorota SZAL[1]
Renata GRUCA-ROKOSZ[2]

HEAVY METAL CONTAMINATION IN SEDIMENTS OF RZESZÓW RESERVOIR (POLAND)

Sediments of Rzeszów Reservoir were characterized by a higher content of zinc compared to other heavy metals (Cu, Cr, Ni and Cd). The strongest correlations between pairs of heavy metals were Cr–Ni, Ni–Zn, Cu–Ni and Cr–Zn, while there was also a clear relationship between the total chromium and nickel content and the pH value, as well as the percentage of organic matter in the sediments (Cr, Zn, Cu, Ni). The content of chromium and copper occurred at levels exceeding the geochemical background, and the sediments could be classified as of purity class 2 (according to the PIG criterion) or class 3 (according to the Müller's classification). Ecotoxicological criteria indicate that levels of chromium, nickel and cadmium could affect aquatic life. However, the heavy metals differ in mobility and bioavailability. The highest percentage of ion exchangeable fraction was recorded for nickel, and the lowest for chromium. This means that sediments have a greater ability to release nickel into the water column, as a result of which they are a secondary source of pollution for the aquatic ecosystem.

Keywords: sediments, heavy metals, bioavailable fractions

1. Introduction

Dam reservoirs are particularly exposed to various types of pollution introduced into the aquatic environment due to their location at the lowest points of the terrain. Therefore, sediments of these reservoirs may provide necessary knowledge about the impact of anthropopressure on the aquatic environment [5]. Heavy metals have a significant share among sediment contaminants, with specific content characterized by: harmfulness and toxicity to living organisms, durability of forms enabling their migration over considerable distances and ability to be included in food chains. Heavy metals are not biodegradable, but

[1] Corresponding author: Dorota Szal, Politechnika Rzeszowska, ul. Powstańców Warszawy 6, 35-959 Rzeszów, d.piwinska@prz.edu.pl, https://orcid.org/0000-0002-3547-0171
[2] Renata Gruca-Rokosz, Politechnika Rzeszowska, ul. Powstańców Warszawy 6, 35-959 Rzeszów, renatagr@prz.edu.pl, https://orcid.org/0000-0001-8222-2480

only biotransformed as a result of complex physicochemical and biological processes occurring in sediments. These processes determine the mobility and bioavailability of heavy metals. The mobility of a given element means its ability, or one of its chemical forms, to move in the environment [2, 7], which may pose a threat to living organisms. The most mobile and bioavailable fraction is the ion exchange fraction. It includes heavy metals adsorbed ion exchange on the surface of the solid phase. Metal ions, held by weak electrostatic bonds, can easily pass into the water column.

For the assessment of the contamination level of sediments, methods of their classification differ in the number of degrees, classes and a factor affecting their threshold values. In all classifications used, the highest class of heavy metals determines the contamination assessment of sediments. The methods of sediment classification can be described as follows:

- classification of sediment quality applied by the Polish Geological Institute (PIG) [1] – distinguishes three qualitative classes of sediments depending on the content of individual elements,
- geoaccumulation index classification [8],
- ecotoxicological criteria – describes indicators such as TEL (Threshold Effects Level), PEL (Probable Effects Level) and LEL (Lowest Effect Level) based on the impact of a particular pollutant on aquatic organisms [15].

The purpose of the research was to determine the content of selected heavy metals in the sediments of the dam reservoir in Rzeszów along with an assessment of their pollution. The share of the bioavailable form was determined using single extraction enabling the extraction of the ion exchange fraction.

2. Materials and methods

The subject of the study were sediments deposited in the dam reservoir in Rzeszów. Sediment samples were collected once in July 2016 using a gravity corer (KC Kajak). The location of 5 sampling stations are shown in Fig. 1, with morphometric parameters of the Reservoir also presented.

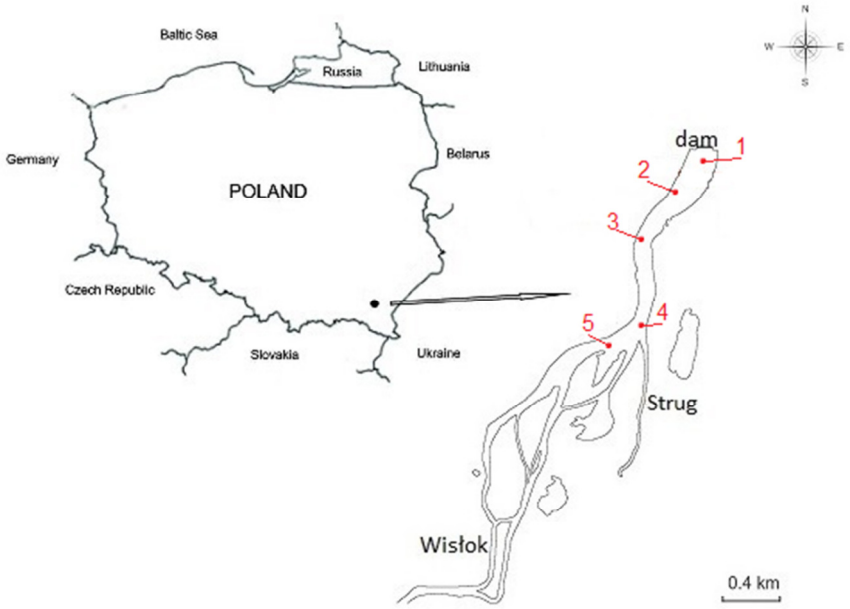

Fig. 1. Rzeszów Reservoir – location of sampling stations and morphometric parameters

The uppermost 5 cm of sediments was sampled for analysis, which were then dried to constant weight at room temperature, and then at 60°C. The sediments were milled, prior to determinations being made for such parameters as: pH, percentage of organic matter (OM), organic carbon (TOC), total nitrogen (TN), carbonates (CO_3^{2-}), as well as metals, including heavy metals Al, Fe, Cr, Cu, Ni, Cd, Zn. Ion–exchangeable fractions within total contents were determined for Cr, Cu, Ni, Cd and Zn.

OM content was determined as loss after drying of sediments within 4 h at 550°C. Reaction was determined potentiometrically (MultiLine P4, WTW, Germany) in slurry with 1N KCl [9]. Carbonate content was measured by volume using the Scheibler apparatus, while TOC and TN contents were determined at 1020°C using a CN elemental analyzer (Flash EA 1112, ThermoQuest). Prior to determination of TOC content, the dried and ground sediment samples were placed in a desiccator with concentrated HCl vapors [19] for 24 h, to ensure the removal of carbonates. Prior to analysis, the sediment sample was again dried to constant weight at 60°C.

To mineralize sediments in order to determine total contents of some heavy metals, portions weighing about 0.5 g were placed into a Teflon vessel and 10 ml of concentrated, spectrally pure nitric acid was then added. Samples were placed into a MARS 6 Microwave Digestion System, and mineralized using microwave energy at 1600 watts for 40 min. at 180°C (temperature rise time – 15 minutes, soaking time – 25 minutes). After cooling, mineralizates were filtered through

quantitative paper filters, and additionally using syringe filters. Heavy metal contents were then determined using a plasma emission spectrometer (ICP–OES GBC Quantima E 1330).

To determine the bioavailable fraction of certain heavy metals, 6 g portions of sediment were shaken with 60 ml of 0.01 mole $CaCl_2$ at room temperature for 2 h [4]. The samples were then centrifuged and filtered through syringe filters. They were analyzed for heavy metal content by the method described above.

3. Results and discussion

Results for chemical parameters of Rzeszów Reservoir sediments are presented in Table 1.

Table 1. Chemical content and selected parameters in the sediments analyzed

Parameter	Unit	Station				
		1	2	3	4	5
pH	–	7.66	7.75	7.78	7.83	7.75
CO_3^{2-}	%	7.54	5.18	4.85	3.47	5.20
OM		9.22	6.40	6.14	4.83	7.55
TOC		2.58	1.56	1.45	1.35	2.20
TN		0.50	0.28	0.22	0.23	0.43
C:N	–	5	6	6	6	5
Fe	%	1.87	1.45	1.45	1.24	1.73
Al		2.37	1.81	1.68	1.31	2.48

Sediments from all the sampling stations were slightly alkaline, with pH values in the 7.66–7.83 range. The lowest value characterized sediments at Station 1, the highest those at Station 4. Contents of carbonate were low, ranging from 3.47% at Station 4 to 7.54% at Station 1. Slightly higher values were obtained in the Besko Reservoir (6.12–13.23%) [13]. In turn, Dobczyce Reservoir sediments are found to have lower abundance of carbonate, in the 0.42–3.18% range [18].

The sediments of Rzeszów Reservoir are also low in organic matter, with contents ranging from 4.83% at Station 4 to 9.22% at Station 1. Organic carbon content (TOC) was found to correlate strongly with OM content (R^2 = 0.92). Sediments were also characterized by a low total nitrogen (TN) content – in the range 0.22% (Station 3) to 0.50% (Station 1). Positive correlations were found between OM and TN content (R^2 = 0.87) as well as between TOC and TN (R^2 = 0.99). For comparison, Besko Reservoir was previously obtained to have OM and TOC in sediments in the 3.88–5.93% and 1.11–1.81% range, respectively [13]. Furthermore, sediments of Włocławek Reservoir have an OM content over twice as high – at 11.5% [16].

C:N ratios in the sediments of Rzeszów Reservoir range from 5 to 6. Values for the C:N ratio indicate a greater share of autochthonous matter in sediments.

Rzeszów Reservoir sediments were characterized by iron contents in the range 1.24–1.87% and by aluminum in the range 1.31–2.48%. The sediment contents of these heavy metals are lowest at Station 4, while the highest values noted for iron and aluminum are at Station 1 and 5, respectively. These values were similar to those obtained in sediments of Besko Reservoir (Fe: 1.88–2.23%, Al: 1.34–1.85%) [13] and Solina Reservoir (Fe: 0.88–1.81%, Al: 0.92–1.86%) [12].

The sediments of Rzeszów Reservoir were also analyzed for their contents of the heavy metals Cr, Cu, Ni, Cd and Zn. The results of this analysis are presented in Fig. 2.

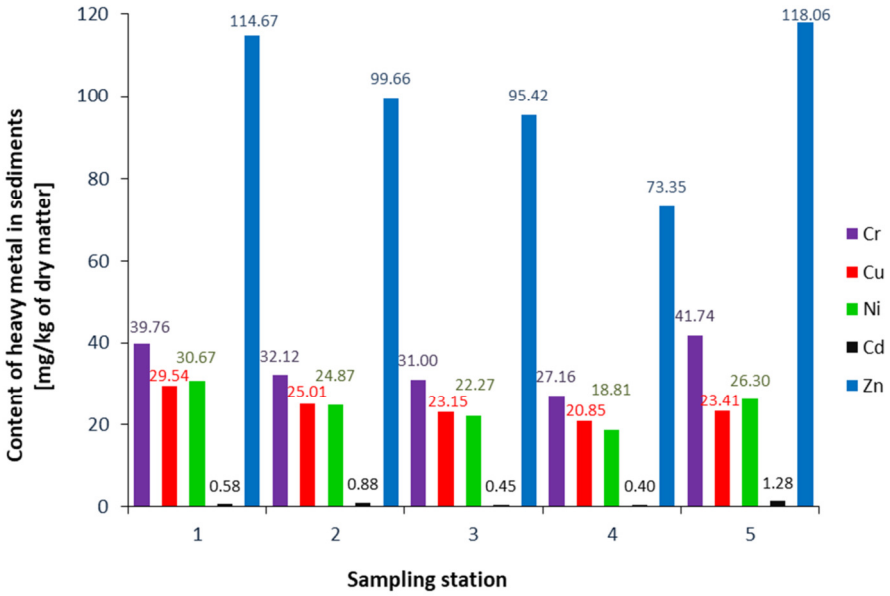

Fig. 2. Contents of heavy metals in sediments of Rzeszów Reservoir

Sediments of Rzeszów Reservoir are characterized by significant contamination by heavy metals, considering the content of zinc (73.35–118.06 mg·kg^{-1} of dry matter). In terms of total content, this element was clearly predominant over the other heavy metals. A similar content of zinc was found in sediments of Solina Reservoir (28.68–144.85 mg·kg^{-1} of dry matter) [12], while lower values were noted for sediments of Zesławice Reservoir (55.0–72.6 mg·kg^{-1} of dry matter) and Krempna Reservoir (39.7–79.5 mg·kg^{-1} of dry matter) [6].

The highest values for R^2 determination coefficients concern the Cr–Ni relationship (0.74), the Ni–Zn relationship (0.81), the Cu–Ni relationship (0.86) and the Cr–Zn relationship (0.92). High correlations between total contents of different heavy metals have also been confirmed by other authors [3, 14]. There was also

a clear relationship between total contents of copper and nickel, and the pH value (pH–Cu: 0.96, pH–Ni: 0.97), as well as the percentage of organic matter in sediments (OM–Cr: 0.78, OM–Zn: 0.79, OM–Cu: 0.81, OM–Ni: 0.97).

According to the classification of river and lake sediments prepared by the Polish Geological Institute (PIG) [1], sediments of Rzeszów Reservoir can be classified as of purity class 2 (medium contamination), mainly due to the highest exceedances of the geochemical background value for chromium and copper. In turn, the application of Müller's criterion [8] evidenced the 3th purity class (i.e. moderately to heavily contaminated sediments), with this again confirmed by observed values for the geoaccumulation index in respect of chromium (2<Igeo<3). Taking into account ecotoxicological criteria, it has been observed that chromium, nickel and cadmium may all be regarded as potentially toxic to living organisms (>LEL, TEL). Possible toxic effects due to zinc do not occur, however (<PEL; no TEL).

Analysis related to overall contents of heavy metals was augmented by considerations of their mobile fractions. The results are as shown in Fig. 3.

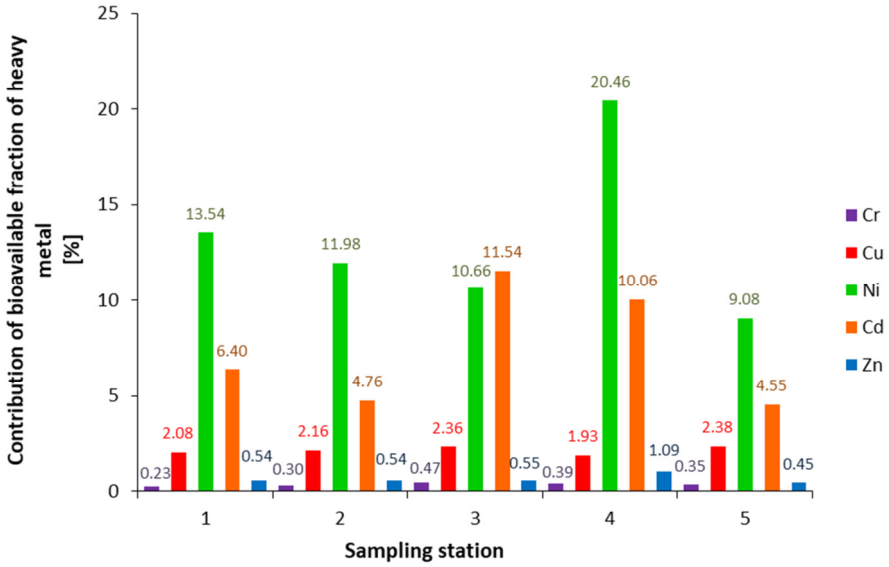

Fig. 3. Bioavailable fractions of heavy metals in sediments of Rzeszów Reservoir

Based on the procedure of extraction of the mobile fraction, it was found that the following hierarchy for the mobility of heavy metals (and hence for the possibility of secondary water contamination in a reservoir) is arranged: Ni>Cd>Cu>Zn>Cr. This order arises percentage amounts of heavy metals in the ion–exchangeable fraction. This fraction is considered the most mobile and the most sensitive to changes in environmental condition in the benthic zone. When quantified contents of the heavy metals are concerned (in mg·kg^{-1}), the ordering is: Zn>Cr>Cu>Ni>Cd.

Largest percentage of the ion–exchangeable fraction was obtained in the case of nickel (in the range 9.08–20.46%). Sediments of River Liwiec has also been characterized by high nickel mobility (15.6%) [10].

The ion–exchangeable fractions within the total contents of chromium, copper and zinc are similar to those in the sediments of Solina Reservoir (Cr, Cu, Zn) [12], the Łasica Canal (Cr, Zn) [11] and the River Utrata (Cu, Zn) [17]. Accurate comparisons with results for other water reservoirs are not entirely possible due to varying methods and extractants used. Most of the previous research [10, 11, 17] has applied extractants other than used in our work ($CaCl_2$).

4. Conclusions

Analysis of sediments from Rzeszów Reservoir in terms of contamination with heavy metals and assessment of potential toxicity to living organisms yields the following conclusions:

- Compared with other heavy metals studied, it was zinc that achieved highest values (73.35–118.06 $mg \cdot kg^{-1}$ of dry matter).
- According to the criteria from the Polish Geological Institute (PIG), sediments at Rzeszów can be classified as of purity class 2 (medium contamination). Where Müller's classification is taken into account, sediments are found to be in the 3th purity class (denoting moderate to strong contamination). While based on ecotoxicity criteria, contents of chromium, copper, nickel and cadmium indicate potential toxicity to living organisms.
- Mobility data for the heavy metals is arranged in a hierarchy Ni>Cd>Cu>Zn>Cr, which means that nickel has the highest mobility than any other heavy metal studied. This element has a greater capacity for release from sediment into the water column and thus – there is a possibility of secondary contamination.
- While results for heavy–metal bioavailability in Rzeszów Reservoir have been compared loosely with those for other aquatic ecosystems. However, an accurate and reliable comparison of these results was not possible due to differences in research procedures applied.

References

[1] Bojakowska I., Sokołowska G., Geochemiczne klasy czystości osadów wodnych, Przegląd Geologiczny, Warszawa, 1998, 46 (1), 49–54.

[2] Gawdzik J., Mobilność metali ciężkich w osadach ściekowych kondycjonowanych chemicznie, nr 5, Gaz, woda i technika sanitarna, 2010, 33–36.

[3] Głosińska G., Sobczyński T., Boszke L., Bierła K., Siepak J., Fractionation of Some Heavy Metals in Bottom Sediments from the Middle Odra River (Germany/Poland), Polish Journal of Environmental Studies, 2005, 14(3), 305–317.

[4] Houba V. J. G., Novozamsky I., Lexmind T. M., van der Lee J. J., Applicability of 0.01 M CaCl2 as a single extraction solution for the assessment of the nutrient status

of soils and other diagnostic purposes, Communications in soil science and plant analysis, 1990, 21, 19–20.

[5] Koś K., Zawisza E., Charakterystyka geotechniczna osadów dennych zbiornika rzeszowskiego, Czasopismo Inżynierii Lądowej, Środowiska i Architektury – Journal of Civil Engineering, Environment and Architecture, JCEEA, t. XXXII, z. 62 (3/II/15), 2015, s. 195–208, DOI: 10.7862/rb.2015.150.

[6] Madeyski M., Tarnawski M., Ocena stanu ekologicznego osadów dennych wybranych małych zbiorników wodnych, Infrastruktura i ekologia terenów wiejskich, 2006, 4(3), 107–116.

[7] Maj K., Koszelnik P., Metody zagospodarowania osadów dennych, Czasopismo Inżynierii Lądowej, Środowiska i Architektury – Journal of Civil Engineering, Environment and Architecture, JCEEA, t. XXXIII, z. 63 (2/I/16), 2016, s. 157–169, DOI: 10.7862/rb.2016.118.

[8] Müller G., Die Schwermetallbelastung der Sedimenten des Neckars und Seiner Nebenflüsse, Chemiker-Zeitung, 1981, 6, 157–164.

[9] Ostrowska A., Gawliński S., Szczubiałka Z., Metody analizy i oceny właściwości gleb i roślin, Instytut Ochrony Środowiska, Warszawa, 1991.

[10] Pakuła K., Jaremko D., Becher M., Zn, Cu i Ni we frakcjach wydzielonych metodą BCR w osadach dennych, Proc. ECOpole, 2012, 6, 641–646.

[11] Pawłowski J., Rozental M., Drzewińska A., Neffe S., Analiza specjacyjna osadów dennych pobranych na terenie Kampinoskiego Parku Narodowego, Vol. LXIII, Nr 4, Biuletyn WAT, 2014, 113–134.

[12] Piwińska D., Gruca-Rokosz R., The content of selected heavy metals and their bioavailable fraction in sediments of Solina Reservoir (Poland), 2018, E3S Web of Conferences 44, 00143, 8 pages.

[13] Piwińska D., Gruca-Rokosz R., Bartoszek L., Czarnota J., Spatial diversity characterising certain chemical substances in sediments of Besko Reservoir, Journal of Ecological Engineering, 2018; 19(1): 104–112, DOI: https://doi.org/10.12911/22998993/79448.

[14] Rozpondek K., Rozpondek R., Pachura P., Analiza toksyczności osadów dennych zbiornika Poraj w aspekcie stopnia zanieczyszczenia metalami ciężkimi, Acta Sci. Pol. Formatio Circumiectus, 2017, 16(2), 33–43.

[15] Smith S. L., MacDonald D. D., Keenleyside K. A., Ingersoll C. G., Field J., A preliminary evaluation of sediment quality assessmentvalues for freshwater ecosystems. J Great Lakes Res., 1996, 22:624–638.

[16] Trojanowska J., Antonowicz J., Właściwości chemiczne osadów dennych jeziora Dołgie Wielkie, Słupskie Prace Biologiczne, 2005, 2, 123–127.

[17] Wojtkowska M., Bogucki J., Wykorzystanie analizy specjacyjnej w monitoringu metali ciężkich w osadach dennych na przykładzie rzeki Utraty, Ochr. Śr., 2012, 34, 43–46.

[18] Wójcik D., Charakterystyka osadów dennych zbiornika zaporowego Dobczyce, Ochrona Środowiska, 1991, 1(42), 31–34.

[19] Zimmermann C. F., Keefe C. W., Bashe J., Determination of carbon and nitrogen in sediments and particulates/coastal waters using elemental analysis. Method 440.0, NER Laboratory, USEPA, Cincinnati, Ohio, 1997.

Przesłano do redakcji: 10.09.2019 r.

CZASOPISMO INŻYNIERII LĄDOWEJ, ŚRODOWISKA I ARCHITEKTURY
JOURNAL OF CIVIL ENGINEERING, ENVIRONMENT AND ARCHITECTURE
JCEEA, t. XXXVI, z. 66 (3/19), lipiec-wrzesień 2019, s. 25-36, DOI:10.7862/rb.2019.15

Marcin KACZMARZYK[1]
Aleksander WAŚNIOWSKI[2]

INTERNAL HEAT LOADS IN LUNARES ANALOGUE PLANETARY BASE – A CASE STUDY

This case study work focuses on recognising and quantifying internal heat sources in the first European analogue planetary base: the recently constructed Polish LUNARES habitat. The paper explains the necessity of conducting analogue space missions prior to an actual manned exploration of the Moon and Mars. Notions of internal heat loads and gains have been elaborated along with their significance for developing space building physics. This paper presents the results of thorough inspection of all internal heat sources, conducted by one of the authors during ICAres-1 Mars analogue mission aboard the LUNARES base. Three main sources of internal heat loads were identified and carefully studied; the habitat's electrical equipment, the crew body heat and their personal appliances. These heat loads were calculated and total internal heat load of the base was established and discussed. The results of this study may serve as a baseline for predicting internal heat loads aboard actual planetary bases.

Keywords: space building physics, internal heat gains, analogue space station, metabolic heat generation

1. Introduction

1.1. Analogue planetary stations

The development of manned space exploration requires an ability to test new technologies and human behavior in safe, controlled conditions, before an actual spaceflight takes place. Analogue planetary stations, also known as analogue planetary bases, analogue extraterrestrial bases or habitats are specially designed facilities, where selected aspects of long term human presence on extraterrestrial bodies may be simulated. In these facilities, technological solutions, procedures and guidelines for future Moon and Mars exploration are

[1] Corresponding author: Marcin Kaczmarzyk, Politechnika Rzeszowska, Zakład Budownictwa Ogólnego, ul. Poznańska 2, 35-959 Rzeszów; tel. +48178651026; kaczmar@prz.edu.pl, ORCID: 0000-0001-5605-5279
[2] Aleksander Waśniowski, Research Development and Medical Manager, LUNARES Mobile Research Station, Space Garden; aleksander.wasniowski@gmail.com

studied and improved. There are several analogue planetary bases in the world, and new ones are developed [1].

1.2. LUNARES

The first analogue habitat in Europe is LUNARES, located at former military airport in Piła, Poland. The habitat became operational in July 2017, beginning fourteen days long analogue Mars mission for 6 - personnel international crew.

LUNARES consists of a spacious central, domed hub called Atrium and eight adjacent modules, including a galley, dormitory, bathroom, storage, operations room, two laboratories and an airlock.

The secondary component of the LUNARES complex is a simulated lunar and martian terrain situated inside a reinforced aircraft hangar. The whole facility has been made completely lightproof to enable studies on human circadian rhythm and plant growth with artificial lighting.

1.3. Internal heat gains

In building physics, internal heat gains refer to heat emitted by all physical phenomena, activities and processes that release sensible and latent heat inside building envelope, but are not a part of building's heating system [2–5]. The most important internal heat sources are occupants body heat, electrical devices (lighting, appliances, office equipment), food preparation and domestic water heating and its consumption. Internal heat gains are expressed in unit energy, usually in MJ or kWh. Mean heat flux from internal heat sources is called internal heat load and is expressed in unit power [W] in terms of whole building or its section, or in unit power per unit floor surface [W/m^2] or in unit power per unit interior volume [W/m^3]. As a byproducts of mentioned phenomena, internal heat gains cannot be controlled without disrupting the function of a building. Internal heat gains increase the temperature of a building interior and may considerably contribute to building's thermal balance, especially in well thermal insulated objects [2,5,6].

1.4. Internal heat gains in extraterrestrial buildings

The settlements to be established on the surface of the Moon or Mars will initially serve as a scientific facilities, so it may be expected, that they will be equipped with a great variety of electrically powered devices. Additional heat will be produced by batteries and life support systems, such as water recovery and atmospheric control systems [7,8]. Moreover, due to extremely high costs of space transportation, these early extraterrestrial buildings would have highly limited volume and floor surface areas. These two factors suggest, that internal heat load per unit volume or unit surface in these buildings may be significantly higher than what we observe in residential or office buildings on Earth. Due to lack of atmosphere (Moon) or very low atmospheric pressure (Mars) both locations

may be considered as highly insulative environments, where heat exchange between building interior and exterior is highly limited [7, 9–13]. In that situation, determination of internal heat gains becomes a matter of great importance.

An opportunity to study internal heat loads in these unusual buildings presented itself during ICAres-1 analogue mission onboard LUNARES habitat, where numerous scientific experiments were being performed. There were, among others: in situ material processing and utilization, plant growth and animal breeding, spare parts 3D printing, electromagnetic radiation measurements, group dynamics monitoring, continuous artificial lighting studies and extravehicular equipment testing. Although LUNARES lacks working life support system, it is well equipped with laboratory and everyday life devices, so studying its internal heat loads offered a reliable insight into future, full scale solutions.

The purpose of this paper was to identify and quantify all internal heat sources onboard LUNARES habitat in order to determine its total internal heat load.

2. Materials and Methods

2.1. Method

Assessment of internal heat load onboard LUNARES was based on:

- performing thorough inspection of all electrical devices inside the station i.e. learning their input power and daily use;
- conducting a survey among crew members, considering their biometrics, physical activities and electrical devices they used during the mission.

The study was performed in October 2017, during ICAres-1 Mars analogue mission. The corresponding author of this paper was one of ICAres-1 crew members and spent fourteen days onboard the station, acting as Structural material specialist and a PR officer. Thanks to this, the authors possessed a first-hand information about the station's inventory use and an actual, everyday mission schedules.

2.2. Questionnaire description

For the purpose of this paper, Information were gathered from crewmembers by specially prepared questionnaires, that addressed following issues:

- their mission assignments, sex, body weight and height;
- daily profile of their physical activities;
- electrical devices brought for personal use or research purposes;
- personal-use electrical devices, laboratory equipment, subsystems or installations that LUNARES lacks for long-term lunar mission (to be addressed in further studies).

We divided internal heat sources of the LUNARES base into three separate categories:

- base equipment;
- crew body heat;
- crew personal devices.

2.3. Heat loads from electrical devices

It was assumed, that all electric energy expended inside the base will be eventually transformed into heat, allowing it to be counted totally as internal heat loads. It was the case even with electrically heated domestic water, which was collected after each shower, dish washing etc. and used as grey water, allowing it to cool down to ambient temperature, releasing its excess heat into habitat interior.

Knowing the value of nominal power input and daily use of selected electrical devices one may calculate their contribution to mean internal heat load:

$$q_{el} = \sum_{i} \frac{P_i \times t_{mean.i}}{24} \; [W] \tag{1}$$

where: q_{el} is daily mean power demand of a group of electrical devices, i.e. its contribution to daily mean internal heat load, P_i is the mean power input of i- device [W], $t_{mean,i}$ is mean time of i- device daily use [h] and 24 is the number of hours per day

Heat loads from a base equipment and personal devices were calculated according to equation 1.

Electrical devices used only outside the habitat during extravehicular activities but recharged indoors, were accounted for according to equation 2.

$$q = \frac{P_{ch} \times t_{ch} \times (1 - \eta_{ch})}{24} \tag{2}$$

where P_{ch} is nominal power of the battery charger, t_{ch} is daily mean time of charging and η_{ch} is energy efficiency of battery charging

Power demand of group dynamics monitoring equipment SocSenSys was established using the experiment description [14,15]

2.4. Heat load from body heat

Calculation of waste body heat emitted to the surroundings by a person bases on their body surface area and on their instantaneous metabolic rate. The latter is expressed in MET units (Metabolic Equivalent of Task) which represents a ratio of the rate at which a person expends energy, while performing given physical activity compared to a reference value, equivalent to the energy expended when sitting idly. By the definition, the reference value $MET_0 = 58.2$ W/m^2 [16].

Total body surface areas for the crew members were calculated using Du Bois formula:

$$BSA = 0{,}007184 \times m^{0{,}425} \times h^{0{,}725}\ [m^2] \tag{3}$$

where: BSA is body surface area [m^2], m is body mass [kg] and h is person's height [cm]

Basing on the data collected in the survey, mission profile of ICAres-1 and its daily schedules, daily physical activities of the crew were divided into three categories. The division and respective values of metabolic rates assumed for our calculations are presented in table 1.

Table 1. Metabolic rates assumed for the ICAres-1 crew

Activity symbol	Activity description	MET range	Average MET
PA-1	sleep, relax	0.8–1.0	0.90
PA-2	light intensity activities	1.6–2.2	1.90
PA-3	exercises and moderate activities	4.0–6.0	5.00

Daily mean heat load from the crew body heat was calculated as:

$$q_{bh} = \sum_{i,j} \frac{BSA_i \times MET_j \times t_{i,j}}{24}\ [W] \tag{4}$$

where BSA_i is body surface area [m^2] of i-person, MET_j is metabolic equivalent of task for j-activity [-], $t_{i,j}$ is daily mean time spent by i-person on j-activity [h], 24 is the number of hours per day because ambient temperature was not the same in every section of the base.

It was assumed, that due to proper adjustments of clothing for a specified activity and ambient temperature, crew members functioned in thermoneutral conditions i.e. they did not expend extra energy to maintain their body temperature. It is worth mentioning, that most EVAs were physically demanding operations, that have been considerably increasing subject's metabolic heat production. That increase lasted some time after returning to the habitat and presented short-time peak in body heat production inside the base. However, these contributions were judged to be negligible for the overall internal heat gain and were not addressed in the calculations. After three days of ICAres-1 mission, one of the crew members must have permanently left the experiment due to personal reasons. For the purpose of This paper, the situation was considered abnormal and unrepresentative, so metabolic heat loads were calculated here for the complete, six-personnel crew.

3. Results

3.1. Base equipment

Tables 2 to 10 presents heat loads from miscellaneous base equipment for each compartment of the base.

Table 2. Heat generation by the workshop equipment

Device	Nominal power input [W]	Daily use [h]	Daily mean heat generation [W]
3d printer	700	12	350.00
Spectrometer	20	2	1.67
EVA radio battery charger	20	2	0.42
magnetometer battery charger	4	0.14	0.002
soldering iron	100	0.083	0.35
Fan (2x)	20	24	20.00
lighting (5x 20W LED lamps)	100	4	16.67
Laptop	60	12	30.00
interior monitoring camera 2x	10	24	10.00
		in total:	429.10

Table 3. Heat generation by the Storage equipment

Device	Nominal power input [W]	Daily use [h]	Daily mean heat generation [W]
lighting (5x 20W LED lamps)	100	4	16.67
Fan (2x)	20	24	20.00
interior monitoring camera 1x	5	24	5.00
		in total:	41.67

Table 4. Heat generation by the Galley equipment

Device	Nominal power input [W]	Daily use [h]	Daily mean heat generation [W]
fluorescent lamp	144	5	30.00
interior monitoring camera 1x	5	24	5.00
microwave	800	0.75	25.00
induction oven	2000	0.25	20.83
projector	60	0.5	1.25
domestic water electric heater	2200	0.033	3.03
Fan (2x)	20	24	20.00
router	30	24	30.00
		in total:	135.11

Table 5. Heat generation by the Dormitory equipment

Device	Nominal power input [W]	Daily use [h]	Daily mean heat generation [W]
fluorescent lamp	144	2	12.00
Fan (2x)	20	24	20.00
interior monitoring camera 1x	5	24	5.00
		in total:	37.00

Table 6. Heat generation by the Operations room equipment

Device	Nominal power input [W]	Daily use [h]	Daily mean heat generation [W]
fluorescent lamp	144	6	36.00
Fan (2x)	20	24	20.00
interior monitoring camera 1x	5	24	5.00
laser printer	800	0.03	1.11
SocSenSys devices	20	24.00	20.00
modem	20	24	20.00
		in total:	102.11

Table 7. Heat generation by the Biolab equipment

Device	Nominal power input [W]	Daily use [h]	Daily mean heat generation [W]
room lighting (3x 20W LED lamps)	60	4	10.00
air compressor	3.5	24	3.50
plant lighting (2x16W LED lamps)	32	24	32.00
plant lighting (3x32W LED lamps)	96	24	96.00
plant lighting (1x10W LED lamps)	10	24	10.00
microcentrifuge (4x)	12	24	12.00
Fan (1x)	10	24	10.00
interior monitoring camera 1x	5	24	5.00
		in total:	178.50

Table 8. Heat generation by the Bathroom equipment

Device	Nominal power input [W]	Daily use [h]	Daily mean heat generation [W]
fluorescent lamp	144	2	12.00
domestic water heater	1500	3	187.50
		in total:	199.50

Table 9. Heat generation by the Atrium equipment

Device	Nominal power input [W]	Daily use [h]	Daily mean heat generation [W]
LCD status monitor	150	24	150.00
interior monitoring camera 1x	5	24	5.00
air dryer	1200	24	1200.00
artificial daylight LEDs	150	24	150.00
airlock status lamps	48	24	48.00
		in total:	1553.00

Table 10. Heat generation by the Airlock equipment

Device	Nominal power input [W]	Daily use [h]	Daily mean heat generation [W]
interior monitoring camera 1x	5	24	5.00
decontamination UV lamps	6	0.5	0.13
		in total:	5.13

Table 11 summarises the most important results from tables 2 to 10 and additionally shows the values recalculated per unit surface and per unit volume. TRC stands for temperature regulated compartment. This position was introduced, because the airlock was not a TRC. Further considerations involves TRCs only.

Table 11. Heat loads from the habitat equipment for separate compartments

Compartment	Mean heat load [W]	Floor surface area [m^2]	Interior volume [m^3]	Mean heat load per unit surface [W/m^2]	Mean heat load per unit volume [W/m^3]
analitical laboratory	429.10	17.20	28.80	24.95	14.90
storage	41.67	13.00	34.40	3.21	1.21
galley	135.11	13.00	30.40	10.39	4.44
dormitory	37.00	19.70	49.20	1.88	0.75
operations room	102.11	19.70	49.20	5.18	2.08
biolab	178.50	8.00	18.30	22.31	9.75
bathroom	199.50	8.00	18.30	24.94	10.90
atrium	1553.00	37.20	150.00	41.75	10.35
airlock	5.13	15.50	34.00	0.33	0.15
total	2681.11	151.30	412.60	17.72	6.50
total TRC	2675.99	135.80	378.60	19.71	7.07

The total heat load from the base equipment equals almost 2.676 W and gives heat load per unit surface as high as 19.71 W/m^2. This value alone constitutes significantly higher heat load, than total internal heat load in residential buildings [2,5,17] or electric devices heat generation in modern, well equipped offices [18].

Considerable differences in heat loads are to be observed between individual compartments. These results reflect the actual thermal comfort issues observed during the mission, when some compartments were being easily overheated, while other ones required increased heating to maintain desired temperature. Such differences in heat loads between compartments require highly effective interior air circulation system to enable proper heat distribution.

3.2. Body heat

Table 12. Presents daily mean body heat production by ICAres-1 crew. The time of daily activities does not sum up to 24h/day due to extravehicular activities performed by the crew.

Table 12. Daily crew activities and body heat generation

Crew member	Body surface area [m^2]	Daily mean time spent at physical activities [h]			Mean waste heat generation [W]
		PA-1	PA-2	PA-3	
A	1.65	8.00	14.00	1.25	159.86
B	1.63	8.00	15.00	0.50	150.79
C	1.89	8.00	15.00	0.50	174.83
D	1.86	8.50	13.50	1.25	177.99
E	1.88	9.00	13.00	1.25	177.97
F	2.25	7.00	13.00	3.25	257.56
				in total:	1099.00

This group of internal heat sources provides a substantial contribution to the total internal heat load. In comparison with terrestrial houses or offices, the studied base is rather moderately occupied, offering 22.6 m^2/person, but is almost constantly fully staffed, what is not the case in most of the buildings on earth. Moreover, noticeable amount of time was being spent by the crew on physical exercises, what elevated average metabolic heat generation aboard the habitat. During the ICAres-1 mission, daily mean metabolic heat load per unit floor surface was 8.09 W/m^2. This situates the result between metabolic heat loads for residential buildings and for offices during working hours [2,18]. However, when daily mean metabolic heat loads per unit floor surface are compared, LUNARES presents noticeably higher value, than either houses or offices.

3.3. Personal devices

The list of crew personal devices and their contributions to internal heat loads are presented in table 13.

All of these devices have either low power demands or were usually rarely used. The total mean heat load from this group of internal heat sources (almost 113 W) is relatively low and have no significant effect on total internal heat load in the base.

Table 13. Heat generation by personal devices

Device	Nominal power input [W]	Mean daily use [h]	Daily mean heat generation [W]
laptop 1	65.00	9.00	24.38
Camera	10.00	2.00	0.83
E-book readere	5.00	0.25	0.05
laptop 2	80.00	6.00	20.00
Camera	10.00	0.50	0.21
smartphone	2.00	0.20	0.02
IR camera	10.00	0.25	0.10
laptop 3	60.00	2.00	5.00
smartphone	2.00	1.00	0.08
laptop 4	80.00	10.00	33.33
mp3 player	5.00	2.00	0.42
laptop 5	65.00	8.00	21.67
laptop 6	70.00	2.00	5.83
smartphone	5.00	5.00	1.04
		in total:	112.96

3.4. Total internal heat load

The table 14. Compares heat loads for all three internal heat sources.

Table 14. Comparison of internal heat loads aboard the LUNARES habitat heat source

Physical quantity	Habitat equipment	Body heat	Personal devices	Total
internal heat load[W]	2675.99	1099.00	112.96	3774.98
internal heat load per unit surface [W/m^2]	19.71	8.09	0.83	27.80
internal heat load per unit volume [W/m^3]	7.07	2.90	0.30	9.97

As suspected the total internal heat load aboard the analogue planetary base LUNARES during ICAres-1 mission went far beyond the values observed in residential buildings and slightly exceeded the value for well-developed offices. In highly insulative environment that value of internal heat loads will require highly efficient thermal control system to maintain interior thermal comfort.

3.5. Additional remarks

It is to be observed, that the LUNARES habitat is not equipped with an actual life support system, interplanetary communication, nor with energy storage solution, that would be mandatory for an actual, solar powered lunar or martian base [7,19]. It is to be suspected, that waste heat generated by these systems will considerably increase station's total internal heat load. Another issue to be addressed in the future is the way we compare internal heat loads. The well-established practice is to calculate heat loads per unit floor surface area. This is a correct approach as long as interior heights of compared buildings remain similar. If, however, living in partial lunar or martian gravity would force significant increase in extraterrestrial buildings' interior heights, using unit volume instead unit surface may turn out to be more suitable basis for comparing internal heat loads.

4. Conclusions

In this paper internal heat sources aboard the LUNARES, an analogue planetary base have been identified and quantified. The calculated total, daily mean internal heat load 27.8 W/m^2 is considerably higher than the value for residential buildings and slightly higher than for well-developed offices. Internal heat loads in an actual extraterrestrial base would be still much higher than the calculated value due to presence of life support, interplanetary communication and energy storage systems, which were absent in the analysed building. While this paper provides reliable assessment of a heat load from appliances and laboratory equipment, total internal heat load of an actual planetary base are to be subject of further studies.

References

[1] Heinicke Ch., Orzechowski L., Abdullah R., von Einem M., Arnhof M.: Updated Design Concepts of the Moon and Mars Base Analogue (MaMBA). EPSC Abstracts 2018 Vol. 12, EPSC2018-599-2, 2018 European Planetary Science Congress 2018.

[2] Coşkun T., Turhan C., Durmuş Arsan Z., Gökçen Akkurt G.: The Importance of Internal Heat Gains for Building Cooling Design. Journal of Thermal Engineering 2017, Vol. 3, No. 1, pp. 1060–1064, January, 2017.

[3] Internal Heat Gain – an overview ScienceDirect Topics, https://www.sciencedirect.com/topics/engineering/internal-heat-gain.

[4] Monstvilas E., Banionis K., Stankevičius V., Karbauskaite J., Bliūdžius R.: Heat gains in buildings – Limit conditions for calculating energy consumption. Journal of Civil Engineering and Management.

[5] Starakiewicz A.: Zużycie nośników energii w budynku jednorodzinnym na cele ogrzewania ciepłej wody użytkowej i potrzeb bytowych, Czasopismo Inżynierii Lądowej, Środowiska i Architektury – Journal of Civil Engineering, Environment and Architecture, JCEEA, 2016, t. XXXIII, z. 63 (3/16), lipiec-wrzesień 2016, s. 439–446, DOI: 10.7862/rb.2016.227.

[6] Elsarrag E., Alhorr Y.: Modelling the thermal energy demand of a Passive-House in the Gulf Region: The impact of thermal insulation. International Journal of Sustainable Built Environment 2012, Volume 1, Issue 1, June 2012, pp. 1–15.

[7] Hanford A. J.: Advanced Life Support Baseline Values and Assumptions Document. NASA/CR-2004-208941.

[8] Life Support Systems – Sustaining Humans Beyond Earth, https://www.nasa.gov/content/life-support-systems.

[9] Simonsen L. J., DeBarro M. J., Farmer J. T.: Conceptual design of a lunar base thermal control system. https://ntrs.nasa.gov/archive/nasa/casi.ntrs.nasa.gov/19930004815.pdf.

[10] Swanson T. D., Radermacher R., Costello F. A., Moore J. S., Mengers D. R.: Low-Temperature Thermal Control. SAE Technical Paper Series 901242.

[11] Sridhar K. R., Gottmann M.: Lunar base thermal control systems using heat pumps, Acta Astronautica 1996, Vol. 39. No. 5, pp. 381–394, 1996, https://doi.org/10.1016/S0094-5765(96)00100-2.

[12] Kaczmarzyk M., Gawroński M., Piątkowski G.: Global database of direct solar radiation at the Moon's surface for lunar engineering purposes E3S Web Conf., 2018 49, 00053 DOI 10.1051/e3sconf/20184900053.

[13] Kaczmarzyk M., Gawroński M., Piątkowski G.: Application of Finite Difference Method for determining lunar regolith diurnal temperature distribution, E3S Web Conf., 2018 49, 00052 DOI 10.1051/e3sconf/20184900052.

[14] Grabowski M. et al.: An Experimental Platform for Quantified Crowd. 24th International Conference on Computer Communication and Networks, ICCCN 2015, Las Vegas, NV, USA, August 3–6, 2015, 2015.

[15] Rüb I., Matraszek M., Konorski P., Perycz M.: 30 Sensors to Mars: Toward Distributed Support Systems for Astronauts in Space Habitats. IEEE 39th International Conference on Distributed Computing Systems (ICDCS 2019).

[16] Manore M., Thompson J.: Sport Nutrition for Health and Performance. Human Kinetics. 2000 ISBN 978-0-87322-939-5.

[17] Neto A., Fiorelli F.: Comparison between detailed model simulation and artificial neural network for forecasting building energy consumption. Energy and Buildings 40 (2008) 2169–2176.

[18] Kim H., Park K., Kim H.Y., Song Y.: Study on Variation of Internal Heat Gain in Office Buildings by Chronology. Energies 2018, 11, 1013.

[19] Landis G. A., Bailey S. G.: Photovoltaic power for a lunar base. Acta Astronautica 1990, vol. 22, pp. 197–203 (1990).

Przesłano do redakcji: 30.09.2019 r.

CZASOPISMO INŻYNIERII LĄDOWEJ, ŚRODOWISKA I ARCHITEKTURY
JOURNAL OF CIVIL ENGINEERING, ENVIRONMENT AND ARCHITECTURE
JCEEA, t. XXXVI, z. 66 (3/19), lipiec-wrzesień 2019, s. 37-45, DOI:10.7862/rb.2019.16

Jakub ŻYWIEC[1]

USING THE WEIBULL ++ SOFTWARE IN WATER SUPPLY NETWORK FAILURE ANALYSIS

The water supply network is a basic element of the water distribution subsystem and its task is to provide consumers with water of appropriate quality, in the required quantity, under appropriate pressure, at any time and at an acceptable price. To fulfil these tasks, the water supply network should have an appropriate level of operational reliability. The paper presents an analysis of the causes of water pipes failures using the Weibull++ software. The analysis was based on the operational data from 2018 obtained from the water supply company. The data included the failure book specifying the date and place of the failure, the cause of the failure, diameter and material of the damaged pipe. The probability density function for the failure of water pipes and its cumulative distribution function have been determined. The impact of individual types of failure causes on the failure of the water supply network was determined. The results provide information about the probability of failures of the water supply network depending on their cause. These results can be used in further analyses of the reliability and safety of water supplies to consumers.

Keywords: failure, reliability, water supply, Weibull++

1. Introduction

The basic element of the water distribution subsystem is the water supply network with utilities, therefore the reliability and security of water supply to the consumer depends mainly on its operation [1,2,3,4,5,6]. The distribution subsystem should be able to provide water of the right quality, in the required quantity, under the right pressure, at any time and with an acceptable price [1,3,6,7]. The biggest threat to the performance of the above tasks are failures of the water supply networks, which may cause interruptions in the water supply or affect water quality, which reduces the reliability and security of water supply to consumers [7,8,9,10,11,12,13,14,15,16]. The causes of water supply network failures may be internal (errors at the stage of design, construction or operation) or external (random failures resulting from the impact of the natural environment

[1] Jakub Żywiec, Politechnika Rzeszowska, Katedra Zaopatrzenia w Wodę i Odprowadzania Ścieków, ul. Powstańców Warszawy 6, 35-959 Rzeszów; tel. +48178651427; j.zywiec@prz.edu.pl. http://orcid.org/0000-0002-0823-4229

or human activity) [2,17]. Water supply companies should strive to reduce the number of breakdowns through appropriate management of the water supply network, carrying out renovation and repair plans, the use of modern operational tools (GIS applications, hydraulic models) and monitoring of the water supply network operation [3,5,7,8,11,12,14,18]. The main purpose of the work is to present the possibilities of using the Weibull ++ software for water supply network failure analysis. The paper attempts to describe the probability distribution model of a water supply network failure by means of a statistical probability distribution. The causes of the water supply network failure were identified and their impact on the failure of the distribution subsystem was examined. An application example was made for real data provided by a water supply company operating in a voivodeship city located in south-eastern Poland. The results of the work will complement the research conducted so far and will provide valuable information for water supply system operators.

2. Research methodology

The Weibull ++ software is a tool for testing the reliability of individual parts, complex machines or entire systems [19]. Input data for the program are operational data such as time between failure (TBF) or time to failure (TTF). These data are described by units of time: minutes, hours, days, but can also be described by other units, e.g. the number of work cycles performed, kilometres travelled, etc. Then the program selects the probability distribution model for the entered data with the assumed method of parameter estimation and the given confidence level. The adjustment and selection of the distribution to the description of the real data is based on the ranking created on the basis of: the result of the Kolmogor-Smirnov test, the normalized correlation coefficient (rho-Spearman) and the logarithmized value of the distribution probability function for the estimated parameters. The matching results may vary depending on the method used to estimate the distribution parameters, i.e. the least squares method, the rank regression method or the maximum likelihood estimation method (MLE). The program has the ability to describe the input data using the following probability distributions: 1-parameter exponential, 2-parameter exponential, normal, logarithmic normal, gamma distribution, g-gamma distribution, logistic, Gumbel or Weibull distribution 1, 2 or 3 -parameter [19]. On the basis of the obtained model, the program gives us the possibility to determine the reliability function R(t) (describing the probability that the object will not be damaged in time t), the failure function F(t) (describing the probability of object damage in time t), the average working time of the object to failure MTTF (Mean Time To Failure), the average object operation time between subsequent failures MTBF (Mean Time Between Failures) and the failure rate function $\lambda(t)$. For each of these functions you can specify confidence limits of a given level,

which are calculated using the methods: FM (Fisher Matrix) or LRB (Likelihood Ratio Bounds). Based on the operational data, the program also allows [19]:

- testing the reliability of the object under varying load and strength conditions,
- comparative analysis of the causes of failures,
- post-warranty data analysis,
- economic analysis for a specified level of object reliability.

The paper attempts to describe the distribution model of the probability of water supply network failure based on data on failures in 2018 and analysis of their causes. In the first step, water supply failures were classified in terms of their cause. Based on the available data, 4 basic types of causes of water supply failures in the analysed Collective Water Supply System (CWSS) are specified: corrosion, unsealing, brake and crack. After the initial analysis, the data were introduced into the Weibull ++ software, in which a probability distribution model describing the failure of the water supply network was created. The described random variable is the network operation time until the failure occurs. After performing preliminary calculations, the program selected the Weibull probability distribution closest to the input data. The estimation of the distribution parameters was performed using the MLE method, which is recommended for use with a large amount of collected data [19]. The 2-parametric Weibull distribution implemented for the analysed data is described by the probability density function (density of the random variable T) taking the form [19,20]:

$$f(t) = \frac{\beta}{\eta} \cdot (\frac{t}{\eta})^{\beta-1} \cdot e^{-(\frac{t}{\eta})^{\beta}} \tag{1}$$

where: β – distribution shape parameter,
η – distribution scale parameter,
t – variable described by the distribution,
e – the Euler number.

Then the program determined the failure function F(t), which characterizes the probability of water supply network failure. It is the distribution function of the random variable T. It is given by the formula [19,20]:

$$F(t) = 1 - e^{-(\frac{t}{\eta})^{\beta}} \tag{2}$$

Similarly, the failure functions of water supply network, characterizing the probability of failure related to a given type of cause, were determined.

For the failure function F(t) confidence limits were set at 99% using the FM method. This means that the numerical value F(t) will be between these limits with a probability of 99%.

3. Research object

The analysis was carried out for the collective water supply system (CWSS) of a voivodeship city located in south-eastern Poland. The total length of the pipes of the examined water supply network is 1025.7 km. The main network (55.1 km) is made of cast iron, steel and polyethylene pipes; the distribution network (605.0 km) is made of cast iron, steel, asbestos-cement, PE and PVC pipes; Water supply connections (365.6 km) are made of steel, PE and PVC pipes. The age structure of the pipes is shown in Figure 1.

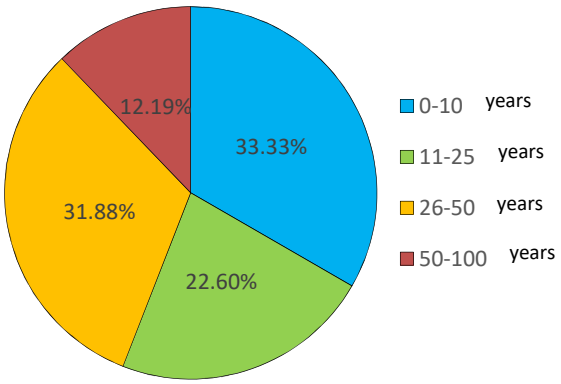

Fig. 1. The age structure of the water supply network pipes

The analysis was performed for real operational data made available by a water supply company. The data included the age structure of the network and the failure log detailing the date of the failure, the location of the failure, the cause of the incident, the diameter and material of the damaged pipe. The network diagram of the analysed CWSS is presented in Figure 2.

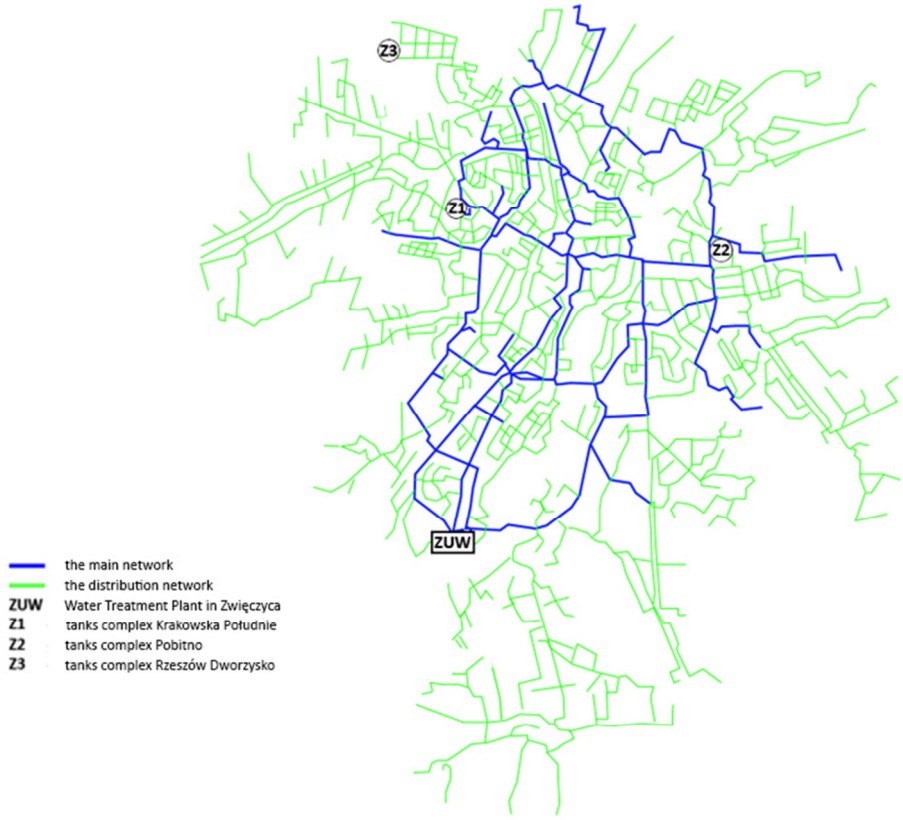

Fig. 2. Scheme of the analysed water supply network

4. Results

During the analysed year 2018, 216 water supply network failures occurred. In the failure log kept by the water supply company the following causes of failure were specified: corrosion, unsealing, cracking and breaking of the pipe. The number of failures due to corrosion of the pipe was 103, which constituted 47.7% of all failures, unsealing was the cause of 83 failures, which corresponded to 38.4% of failures, 22 failures were due to a broken pipe - 10.2%, and failures caused by pipe crack occurred only 8 times, which accounted for 3.7%.

Figure 3 presents the density probability function of the water supply network in the analysed year 2018 described by equation 1, for which the Weibull distribution parameters were calculated, i.e. the shape parameter $\beta = 1.55301$ and the scale parameter $\eta = 229.090797$. The function describing the density of the probability distribution takes the form:

$$f(t) = \frac{1{,}55301}{229{,}090797} \cdot \left(\frac{t}{229{,}090797}\right)^{1{,}55301-1} \cdot e^{-\left(\frac{t}{229{,}090797}\right)^{1{,}55301}}$$

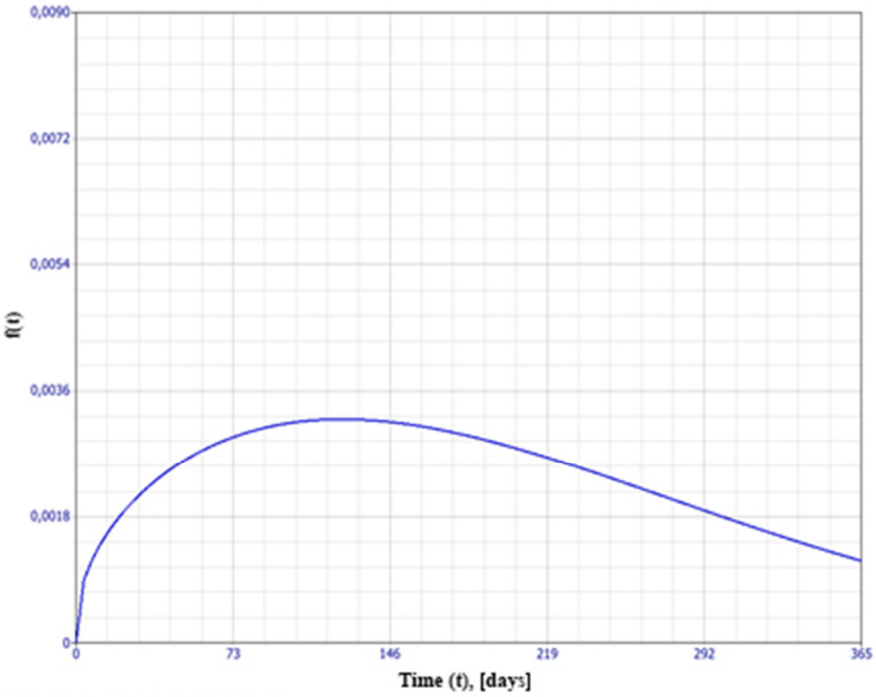

Fig. 3. Probability density function describing the failure of the water supply network

The density function of the probability distribution describes us a random variable, which is the working time until failure. The field below the graph determines the probability of a water supply network failure. We can calculate it as the integral of f(t) in the range (0,t). At the end of the analysed period (t = 365 days) it was 0.8876791.

Figure 4 presents the cumulative distribution function of random variable t, so we can determine the probability of network damage at a given time t. It is described by equation 2, which after inserting the calculated parameters took the form:

$$F(t) = 1 - e^{-(\frac{t}{229{,}090797})^{1{,}55301}}$$

The cumulative distribution function (blue) is limited from above and below by dashed lines (red) which are the limits of confidence intervals at 99% level. This means that with 99% probability the value of the function F(t) will be between these lines.

Figure 4 also presents the graphs of the failure function F(t) describing the probability of a water supply network failure related to individual types of causes, the equations of which took the form:

- the network failure function related to pipe corrosion:

$$F(t)_C = 1 - e^{-(\frac{t}{357{,}390582})^{1{,}748704}}$$

- the network failure function related to unsealed pipes:

$$F(t)_U = 1 - e^{-(\frac{t}{445{,}433037})^{1{,}413579}}$$

- the network failure function related to pipes break:

$$F(t)_B = 1 - e^{-(\frac{t}{1586{,}524704})^{1{,}135663}}$$

- the network failure function related to pipes crack:

$$F(t)_C = 1 - e^{-(\frac{t}{686{,}716892})^{3{,}446719}}$$

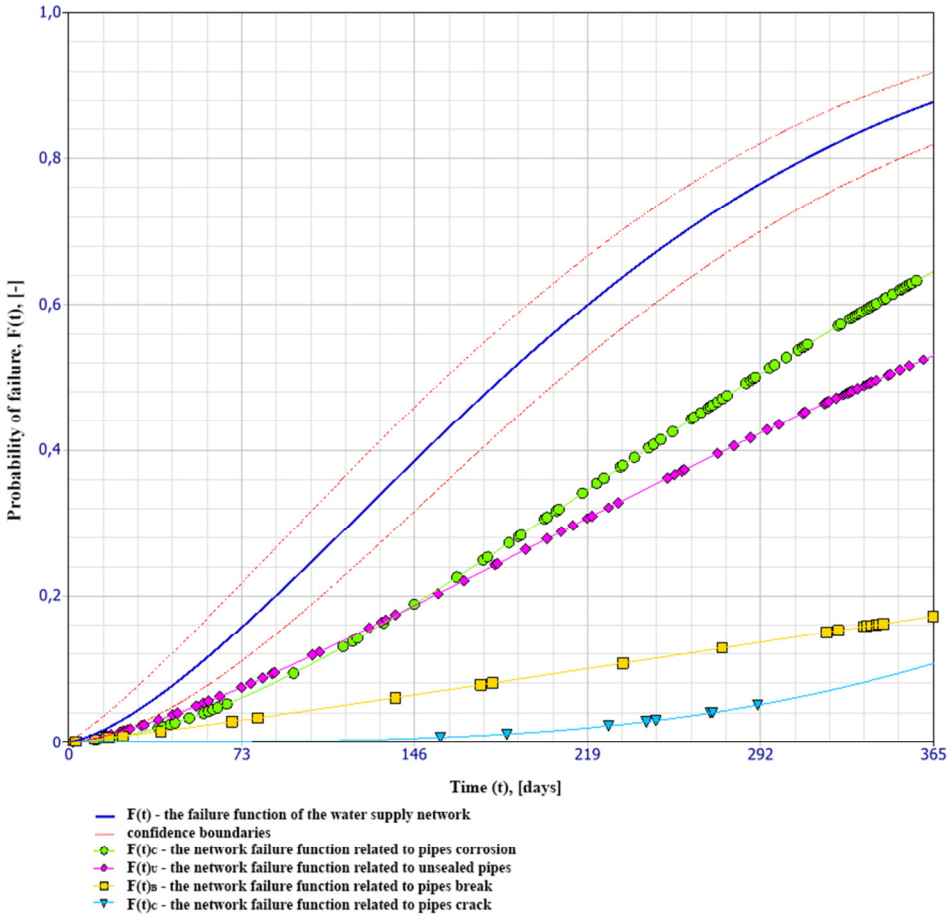

Fig. 4. Graph of the failure function F(t) of the water supply network due to the causes of the failure

The function of network failure due to corrosion ($F(t)_C$) is described in green, due to unsealed pipes in violet ($F(t)_U$), due to pipes break ($F(t)_B$) in yellow and due to pipes crack ($F(t)_C$) light blue. Failures due to corrosion and unsealing had the greatest impact on the water supply network failure function F(t). It was observed that in the first half of the year failures caused by unsealing had a dominant impact on the shape of the graph of the network failure function F(t), while in the second half of the year the shape of the graph was more dependent on corrosion-related failures. Due to the small number of failures associated with broken and cracked pipes, they had a negligible impact on the water supply network failure function F(t).

5. Summary

The paper presents the possibilities of using the Weibull ++ software in the analysis of water supply failure. This program allows testing reliability and failure rates based on statistical probability distributions. The program describes the density probability function of the water supply network based on actual operational data. The developed probability model was based on a 2-parameter Weibull distribution that was matched to real data using the MLE method. On its basis, the failure function of the water supply network F(t) was determined, the value of which determines the probability of failure at a given time t. Based on the data, the causes of the failure include: corrosion of pipe, unsealing, break or crack of pipe. Then, using the program, the failure functions were determined, depending on the cause of the failure ($F(t)_C$, $F(t)_U$, $F(t)_B$, $F(t)_C$), thanks to which it is possible to determine the probability of failure occurrence at time t due to a given cause. These results can be used in further analyses of the reliability and security of water supply to consumers. To assess the failure rate of the water supply network which is a linear object, the failure rate index λ is used, which specifies the number of failures that occur in a unit of time per length of the network. The Weibull ++ software only allows to determine the failure rate function λ (t), which determines the conditional probability of failure occurrence in the time interval Δt, if at the beginning of this interval the tested object was in working order. Further research should explore other options for using the Weibull +software in analysing the reliability and failure rate of collective water supply systems.

References

[1] Budziło B.: Niezawodność wybranych systemów zaopatrzenia w wodę w południowej Polsce. Wydawnictwo Politechniki Krakowskiej, Kraków, 2010.

[2] Kwietniewski M., Rak J.: Niezawodność infrastruktury wodociągowej i kanalizacyjnej w Polsce. Komitet Inżynierii Lądowej i Wodnej PAN, Warszawa, 2010.

[3] Pietrucha-Urbanik K., Pociask K.: Analysis and assessment of water distribution subsystem failure, Journal of Konbin, 2016, 40(1), s. 47–62.

[4] Rak J., Tchorzewska-Cieślak B., Studziński J.: Bezpieczeństwo systemów zbiorowego zaopatrzenia w wodę, Instytut Badań Systemowych, PAN, Warszawa, 2013.

[5] Tchórzewska-Cieślak B., Szpak D., Piegdon I., Szlachta A.: Analysis of selected reliability indicators of water supply network, Journal of Konbin, 2018, 47/1, s. 45–65.

[6] Wieczysty A. : Niezawodność systemów wodociągowych i kanalizacyjnych. t.1. Teoria niezawodności i jej zastosowania, Wydawnictwo Politechniki Krakowskiej, Kraków, 1990.

[7] Tchórzewska-Cieślak B., Szpak D., Piegdon I., Szlachta A.: Quality analysis of water network failure, Journal of Konbin, 2018, 47/1, s. 67–85.

[8] Boryczko K., Tchórzewska-Cieślak B.: Analysis and assessment of the risk of lack of water supply using the EPANET program, Environmental Engineering IV – Proceedings of the Conference on Environmental Engineering IV, 2013, s. 63–68.

[9] Gouglidis A., König S., Green B., Rossegger K., Hutchison D.: Protecting water utility networks from advanced persistent threats: A case study, Static and Dynamic Game Theory: Foundations and Applications, 2018, s. 313–333.

[10] Iwanek M., Kowalska B., Kowalski D., Kwietniewski M., Miszta-Kruk K., Mikołajuk P.: Wpływ różnych czynników na awaryjność sieci wodociągowej w układzie przestrzennym – studium przypadku. Czasopismo Inżynierii Lądowej, Środowiska i Architektury JCEEA, t. XXXII, z. 62/2015, s. 167–183, DOI: 10.7862/rb.2015.12.

[11] Iwanejko R., Bajer J.: Wybrane modele oceny i prognozowania uszkadzalności sieci wodociągowej, Gaz, Woda i Technika Sanitarna, 2012, s. 429–432.

[12] Knapik K., Wierzbicki R., Wieczysty A.: Metody oceny niezawodności podsystemu dystrybucji wody, Zbiór monografii pod redakcja A. Wieczystego Metody oceny i podnoszenia niezawodno sci działania komunalnych sysytemów zaopatrzenia w wodę. Kraków, 2001, s. 365–406.

[13] Kowalski D., Miszta-Kruk K.: Failure of water supply networks in selected Polish towns based on the field reliability tests. Engineering Failure Analysis 35/2013, s. 736–742.

[14] Królikowska, J., Królikowski, A.: Applying the treedendrical scheme failure method to evaluate the reliability of sewage collection draining reliability evaluation subsystems, Environmental Engineering III, 2010, s. 191–195.

[15] Nawrocki J., Świetlik J.: Analiza zjawiska korozji w sieciach wodociągowych, Czasopismo Ochrona środowiska, vol. 33/4, s. 27–40.

[16] Pietrucha-Urbanik K., Studziński A.: Qualitative analysis of the failure risk of water pipes in terms of water supply safety, Engineering Failure Analysis, 2019, 95, s. 371–378.

[17] Bergel T.: Awaryjność sieci wodociągowych małych wodociągów grupowych w Polsce. Gaz, woda i technika sanitarna. 12/2012, s. 536–538.

[18] Piegdoń I., Tchórzewska-Cieślak B., Szpak D.: The use of geographical information system in the analysis of risk of failure of water supply network Environmental Engineering V – Proceedings of the 5th National Congress of Environmental Engineering, 2017, s. 7–14.

[19] Life Data Analysis Reference, ReliaSoft Publishing, 2008.

[20] Kwietniewski M., Roman M., Kłoss-Trębaczkiewicz H.: Niezawdoność wodociągów i kanalizacji, Arkady, Warszawa, 1993.

Przesłano do redakcji: 10.09.2019 r

CZASOPISMO INŻYNIERII LĄDOWEJ, ŚRODOWISKA I ARCHITEKTURY
JOURNAL OF CIVIL ENGINEERING, ENVIRONMENT AND ARCHITECTURE
JCEEA, t. XXXVI, z. 66 (3/19), lipiec-wrzesień 2019, s. 47-64, DOI:10.7862/rb.2019.17

Rafał BUDZIŃSKI[1]

NUMERICAL ANALYSIS OF CABLE NET STRUCTURE WITH APPLICATION OF DIFFERENT PRETENSIONING METHODS

Tension roofs based on cable systems are suitable for covering long span buildings. Such structures are considered to be economic, modern and aesthetic solutions in various multi-functional arenas. Development of materials and construction technologies resulted in an increased number of applications of cable systems in recent years. However, the origin of such structures dates back to 1953, when the cable net supported roof over Raleigh Arena in North Carolina was completed. Designed as self-balanced, the system was eventually pretensioned in order to provide greater stiffness. This implementation became an indispensable part of cable nets construction. A unique method of pretension was applied in one of the first and most recognizable Polish examples of tensile structure, which is the cable net roof over the open-air theater in Koszalin. The system was pretensioned through the outward rotation of simply supported edge arches, which induced tensile forces in roof cables. This simple and effective concept became an inspiration for the introduced study, which focused on the numerical application of such a solution. In this paper, the results of comparative finite element analysis of introduced cable net structure with different methods of pretensioning are presented. The investigation was preceded by the analysis of net shape, concentrated on the value of cable sags in the saddle point of parabolic hyperboloid surface. Effectiveness of the presented solutions was assessed through comparison of internal forces distribution and model deformation. Numerical verification of consecutive concepts led to a gradual reduction of directly prestressed members from 16 suspension cables to 6 cable stays in the analysed roof.

Keywords: tensile structure, parabolic hyperboloid, long span roofs, structure shaping

1. Introduction

The beginning of the 21st century brought a dynamic increase of public investments in sport and cultural infrastructure in Poland. This trend is represented by numerous structures built from scratch as new facilities or as

[1] Rafał Budziński, Rzeszow University of Technology, Department of Building Structures, 2 Poznańska Street, 35-959 Rzeszów; tel. 178651610; r.budzinski@prz.edu.pl. http://orcid.org/0000-0002-9890-845X

a modernization parts in existing venues. Functional and utility requirements for such projects impose a set of attributes that a design should incorporate. These necessities indicate the development of technical solutions that can be effectively implemented in modern arenas. Some major investments in recent years showed an increasing number of applications based on tensile structures, which are successfully implemented in long span buildings. These type of structures gained favor in terms of aesthetics, modernity and economics as a solution for roofs in covered stadiums, sports halls or various multi-arenas [1–5].

Cable roof structures, which are considered as tensile structures, appear in various arrangements. They can be supported by different systems based on:

- simply suspended cables (Fig. 1.a),
- pretensioned cable beams (Fig. 1.b),
- pretensioned cable nets (Fig. 1.c).

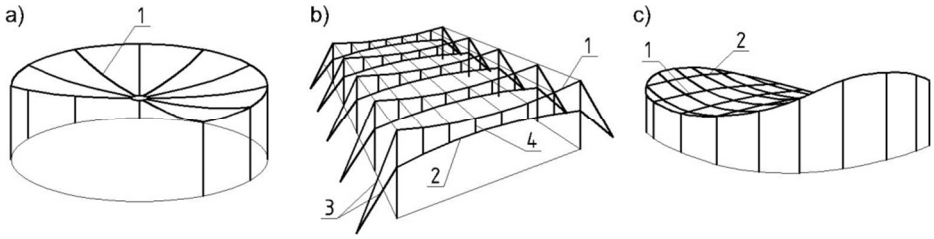

Fig. 1. Examples of different types of tension roof structures (description in the text):
1 – suspension cables, 2 – pretension cables, 3 – stays, 4 – ties

The first two could be designed in different arrangements, which generally comes to radial and parallel planes (Fig. 1.a-b). The last of the mentioned types is based on a cable net, which takes the shape of second order surfaces (Fig. 1.c). This kind of structure, as well as the cable beams, must be pretensioned. In such cases, the pretension provides balance in the static model, which consists of two sets of cables. The suspension cables are intended to transfer loads, while the pretension cables with opposite curvature, ensure stiffness of the system. The general idea of pretensioning the cable structures comes from their high flexibility. The intensity of pretension forces should be adjusted to provide balance and proper stiffness in a specific system [1, 2].

The concept of pretensioning was successfully implemented in one of the first most recognizable tensile structures, which is Raleigh Arena in North Carolina, USA. The structure of the building, which was completed in 1953, was not intended to be primarily pretensioned. The operation was performed to counteract large deformations, which was followed by intrusive noises [6]. Latter studies of such systems helped to develop various solutions in the cable based systems, built in many countries. Apart from the recent expansion of tension roof structures, there has been few examples that can be considered as pioneering applications of such systems in Poland. The roof over the open-air

theatre in Koszalin is one of the representative cases of a pretensioned cable net system. The structure was designed in the shape of parabolic hyperboloid, comparable to the previously discussed arena. However, in this case, the pretension forces were applied through a unique method. The tensioning of the roof cables was achieved by the external rotation of simply supported edge arches, controlled by shortening the cable stays [3–5]. The structure was completed in 1975 and still fulfils its function. This design problem was studied and solved on the grounds of model experiments and partial numerical calculations [3, 7].

Analytical study of the behaviour of cable structures is a complex problem, in which the intensity and method of pretension are followed by many other variables. The complexity of such designs is escalated by the non-linear behaviour of cable members. Furthermore, the response of a certain system is influenced by the flexibility of edge structure. The assumption of ideally rigid supporting members might lead to unreliable results in terms of internal forces and deformations [1, 2]. Various analytical methods evolved and were applied throughout the history of cable roof structures [8]. Recent development of numerical analysis software gives opportunities to solve such design problems. These programmes provide tools for investigating sophisticated cable-based structures with a multi-parameter approach [3].

The aim of this article is to present results of analytical study, in which various simulations of cable pretensioning were performed in several numerical models of a cable net structure. The major part of the analysis was focused on the numerical application of pretensioning method inspired by the completion of the open-air theatre roof in Koszalin. This solution is further referred to as "indirect pretensioning". The study of this phenomenon was preceded by the net shaping analysis. The selected geometry formed the basis for models in the main part of the study, in which indirect pretensioning was applied. The assessment of the introduced solutions was based on the comparison of numerical analysis results, which are represented by several diagrams and summary of internal forces and deformation.

Although the case of the application of indirect pretensioning in open-air theatre roof in Koszalin is widely described in the domestic literature [3–5], a detailed discussion or study of this phenomenon cannot be found. There are few publications that focus on the general behavior of this venue [7, 9], excluding the study of the indirect pretension effects.

2. Scope and methods of analysis

2.1. Scope of the study

The study involved a numerical analysis of several cable net structure variants, designed in the shape of parabolic hyperboloid. The concepts differed

in the curvature of the cables and the method of pretensioning. The finite element analysis was performed with Autodesk Robot Structural Analysis software. The analytical study of structural models was divided into two stages.

The first stage of the study was carried out to select a more effective net shaping related to the value of cable sags. Different functions were used to vary the curvature geometry, which was expected to affect the internal forces and deformation of the net and the edge structure.

The second stage included the study of the selected cable structure with an application of indirect pretensioning method. This step involved the modification of the structure supports and implementation of cable stays. In opposition to the system inspired by the venue in Koszalin, an alternative concept based on the application of indirect pretensioning was introduced.

2.2. Geometric parameters of structures

The analysed structure was designed as a cable net system, which can fulfill the function of a roof over an open-air arena. The cable net formed a shape of parabolic hyperboloid in space and took an oval shape in plan view. The covered area was determined by the maximum theoretical width and length of the structure in plane, which was 36.9 and 71.0 meters, respectively.

The overall dimensions of the roof arose from the edge structure, which was similar in all variants. It consisted of two circular arch-curved beams made of CHS 914x25 sections, with 19.0 m rise and 71.0 m span. The arches were inclined at an angle of 30 degrees to the horizontal plane. The members were initially spaced 4.0 m apart in supporting points, considering the technological aspects of foundation (Fig. 2.a). For the purposes of numerical analysis, the arches were lengthened to the points of intersection, which created two supporting points.

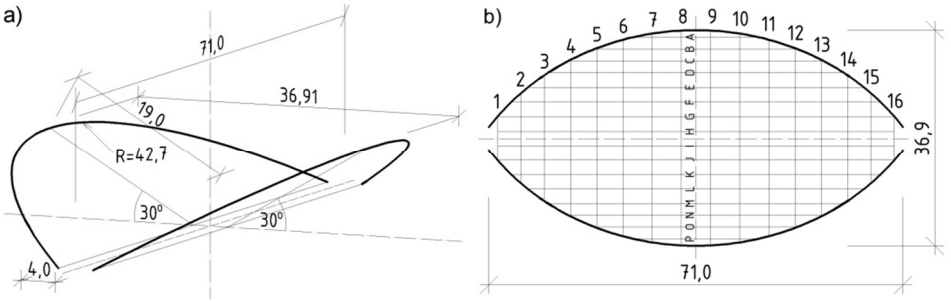

Fig. 2. The structural arrangement of the a) edge arches in axsonometric view and b) cable net system in plan view

The cable net arrangement in plan view was similar in all concepts. It consisted of sixteen suspension cables and sixteen pretension cables, oriented in transverse and longitudinal direction, respectively (Fig. 2.b). The structural

system induced natural sag of suspension cables and the opposite curvature of pretension cables. The cross-sections for these groups were varied. Fully locked cables with a diameter of 50 mm and IPE 160 sections were assigned to suspension and pretension members, respectively. The application of rigid profiles was inspired by the construction of open-air theatre roof in Koszalin. This solution was investigated in a research paper [7], in which the implementation of I-profiles was assessed positively in terms of the impact on global behavior of system under snow load.

The structure selected for the second stage of the analysis was implemented with stays or columns, depending on the variant. These members supported the edge beams and provided self-balance for the structure. Cables with a diameter of 50 mm were adopted for stays. The columns were built from CHS 914x25 members. The summary of cross-sections for all structural members is presented in Table 1.

Table 1. Summary of cross-sections adopted for structural members

Type of member	**Profile/ Section**	**Area of cross-section**	**Moment of inertia about horizontal axis**	**Moment of inertia about vertical axis**
		A	I_y	I_z
		[$\times 10^2$ mm^2]	[$\times 10^4$ mm^4]	[$\times 10^4$ mm^4]
Pretension cables	IPE 160	20.1	869	68.3
Suspension cables	Ø50 cable	16.5	-	-
Edge beams	CHS 914x25	698.22	690317	690317
Stays	Ø50 cable	16.5	-	-
Columns	CHS 159x10	46.8	1305	1305

2.3. Load application

Limited number of load types was introduced in order to investigate and compare the effects of pretensioning in the analysed structures. The cable roof system was subjected to:

- Pretensioning forces “P”,
- Dead load “G”,
- Snow load “S”.

The pretensioning of the cable net system was introduced as “P” load case. The pretensioning forces application was done through initial shortening of the cable specified by the relative dilatation command in the software. In the first stage of the study, in which comparative analysis of the net shaping was carried out, pretensioning forces were directly applied to sixteen suspension roof cables. In the second stage, where the phenomenon of indirect pretensioning was investigated, the forces were subjected only to the implemented cable stays. This action was performed to induce the outward rotation of simply supported edge arches and resulted in pretension of the roof cables.

The dead load, involving the weight of roof construction materials and the structure, was presented as "G" case. The uniformly distributed load applied to the roof was estimated on the basis of the designed roofing layers. The characteristic value of this surface load equaled 0.22 kN/m^2. The weight load of structural members was generated automatically in the software on the grounds of the defined cross sections.

The snow load "S" was represented by downward load applied to the roof surface. Due to complicated geometry of the roof, the shape and value of snow load was approximated from formulas dedicated to mono-pitched roofs. It was defined by uniformly distributed surface load acting on the whole surface of the roof. The load value was calculated assuming the 3rd snow zone specified in the National Annex of EN 1991-1-3 and maximum value of shape coefficient [10]. As a result, the characteristic value of snow load equaled 0.96 kN/m^2.

2.4. Materials and methods of numerical analysis

The numerical models of the structures were built from two types of elements. The cable members were modelled as cable type element provided by the Autodesk Robot Structural Analysis. These kind of elements had no flexural or compressive stiffness and transferred tensile forces only. They obtained simple connections on the ends by default in the model. Bar elements were used in other members, which possessed certain flexural stiffness. The structure was modelled segmentally, where the number and length of elements resulted from the arrangement of nodes in the cable net.

The linear elastic model of steel was adopted for all members in the structure. The yield point of the steel was set at 355 MPa for bar and 870 MPa for cable elements. Young's modulus assigned to cable and bar elements equaled 160 and 210 GPa, respectively.

The response of structural models was received through non-linear analysis applied in Autodesk Robot Structural Analysis. The analysis included the second-order and third-order effects by utilizing P-delta and large displacement options in the software. The calculations were performed using incremental method with 30 load increments and maximum of 40 iterations for one increment. The non-linear problem was solved with the Full Newton-Raphson method, defined by the maximum update after each subdivision and iteration. In order to improve the convergence of the method, the "line search" algorithm with maximum of 5 trials was used.

2.5. Basis of comparison

The study was divided into two parts, in which different attributes were investigated. The comparison of concepts on each stage of analysis was carried out on the basis of internal forces distribution, form of deformation and numerical model stability.

The comparative study of concepts focused on the results obtained from two cases of loading:

- characteristic value of pretensioning forces (1.0P),
- characteristic combination of introduced loads (1.0P+1.0G+1.0S).

For the purposes of the analytical study, the "P" load case was detached from dead load "G", despite standard recommendations [11]. On this basis, the impact of various pretensioning and effects of further gravity load inclusion were investigated separately. The characteristic load combination was introduced to obtain the actual displacement values, which played a crucial role in the analysis of results. In order to limit the number of the presented cases, the design load combination was omitted in the study.

3. Analysis of cable net shape

3.1. Determination of net shape

The investigation of indirect pretension application was preceded by the comparative analysis of net shaping. At this stage, pretension of the structures was achieved by direct application of initial forces to the roof suspension cables. The edge arches were fixed at both ends, which provided the self-balance for the structure. Two concepts of net geometry differing in the value of sags were considered.

The first geometry was determined on the basis of the assumed sag equaled 2.5 m in the saddle point of the surface. This value represented the sag of the longest suspension cables no. 8 and 9, which were anchored close to the keystones of the edge arches (Fig. 1.b). Consequently, the calculated sag-to-span ratio is approximate to the upper recommended limit of 6% [1]. The suspension cable geometry was defined by the catenary curve (Fig. 3), which was described by the formula:

$$f(y) = z = a \cdot \cosh\left(\frac{y}{a}\right) = a \cdot \frac{e^{\frac{y}{a}} + e^{-\frac{y}{a}}}{2} \tag{1}$$

where the value of parameter a was estimated iteratively according to the assumed sag of the longest cable from the equation:

$$f_1 = f(y) - a = a \cdot \cosh\left(\frac{y}{a}\right) - a = a \cdot \frac{e^{\frac{y}{a}} + e^{-\frac{y}{a}}}{2} - a \tag{2}$$

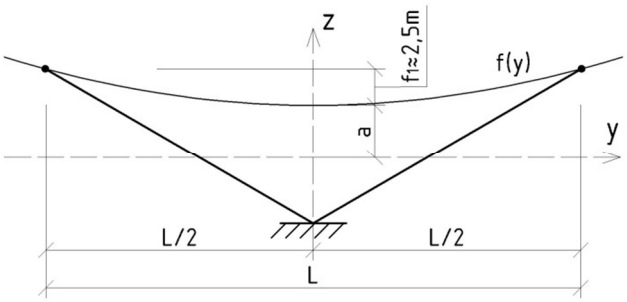

Fig. 3. Determination of the cable curve for the 1st concept of net shaping

The geometry of other suspension cables was obtained through rescaling of the cable curve obtained for the longest members. The curvature of pretension cables resulted from the suspension cable shaping, which set the vertical position of the net nodes. The structural model of the 1st net shaping concept is presented in Fig. 4.

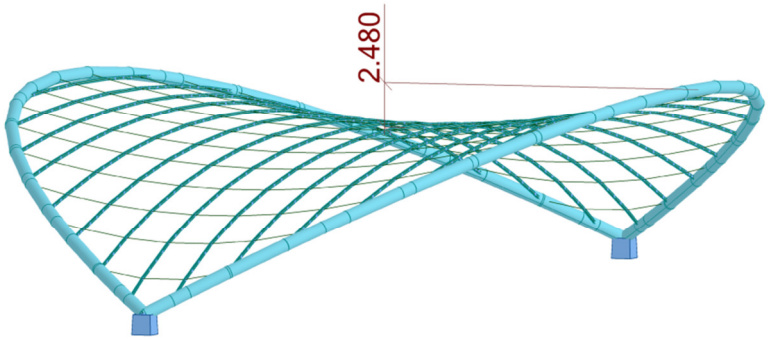

Fig. 4. View of the structural model without roof panels representing the 1st concept of net shaping

In the second concept, net geometry was determined to obtain a curvature of suspension cables so that the planes of the edge arches were tangent to them in the anchor points (Fig. 5). The aim of this action was to eliminate the out of plane bending of the arches, which depended on the direction of the forces transferred from the suspension cables. Considering the nonlinear behaviour of cable members, a certain reduction of the bending moments was expected. In this case, the suspension cable geometry was defined by the parabola curve (Fig. 5), which was described by the formula:

$$f(y) = z = a \cdot y^2 \tag{3}$$

where a was calculated on the basis of the assumed tangency point from the derivative of the parabola function:

$$f'(y) = \frac{dz}{dy} = 2ay = tg(\alpha) \tag{4}$$

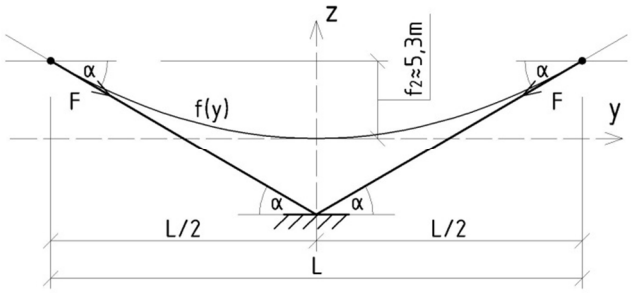

Fig. 5. Determination of the cable curve for the 2nd concept of net shaping

The sag of the longest cable in the saddle point was calculated from the equation (4) and approximate to 5.3 m. As in the previous concept, the geometry of pretension cables resulted from the determination of suspension cables shape. The structural model of the 2nd concept of geometry is shown in Fig. 6.

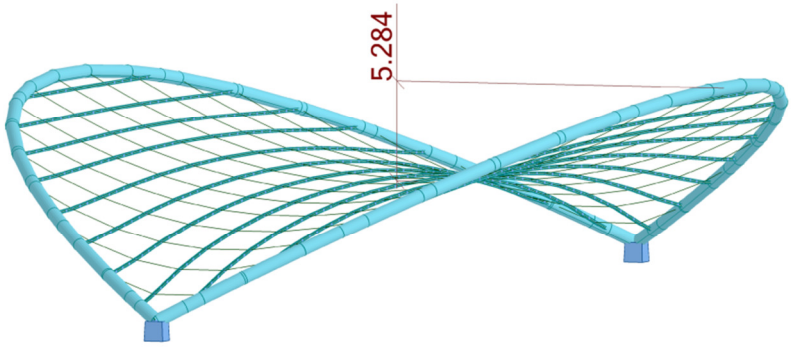

Fig. 6. View of the structural model without roof panels representing the 2nd concept of net shaping

3.2. Assumptions of pretensioning

The comparison between different net shaping was made on the assumption of approximately similar axial forces in the suspension cables under load combination. It was achieved by adjusting the values of initial shortening of the considered members. In this regard, the values of relative dilatation (shortening) for all 16 suspension cables varied between:

- 0.005 ÷ 0.012 in the 1st net concept;
- 0.0008 ÷ 0.0012 in the 2nd net concept.

3.3. Results

Several diagrams of internal forces and deformation for suspension cables and edge beams, considering the 1st and 2nd concept of net shaping are presented in Fig. 7–11. The summary of internal forces and displacement values are given in Table 2.

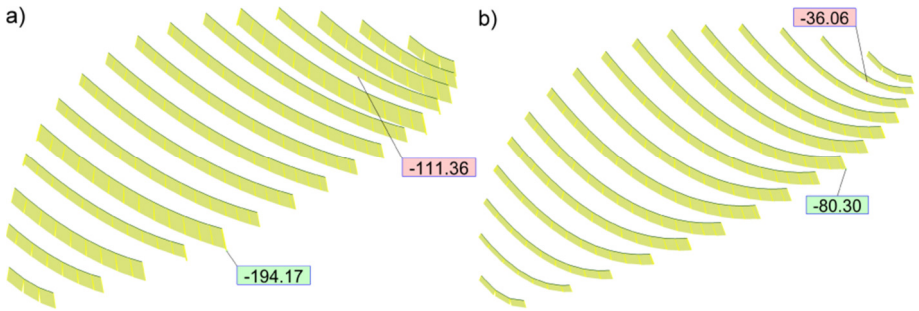

Fig. 7. Axial forces N_X in suspension cables for a) 1st and b) 2nd net shape (1.0P)

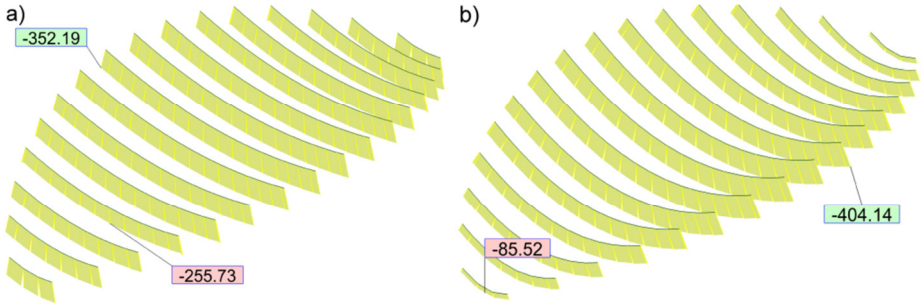

Fig. 8. Axial forces N_X in suspension cables for a) 1st and b) 2nd net shape (1.0P+1.0G+1.0S)

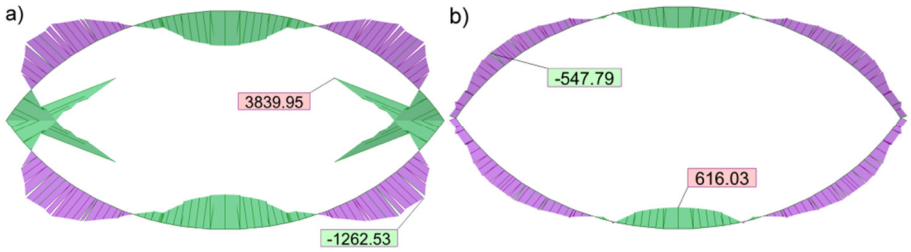

Fig. 9. In plane bending moments M_Y in edge beams for a) 1st and b) 2nd net shape (1.0P+1.0G+1.0S)

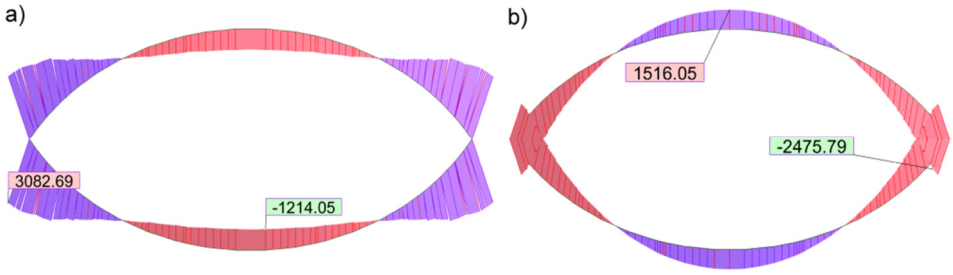

Fig. 10. Out of plane bending moments M_Z in edge beams for a) 1st and b) 2nd net shape (1.0P+1.0G+1.0S)

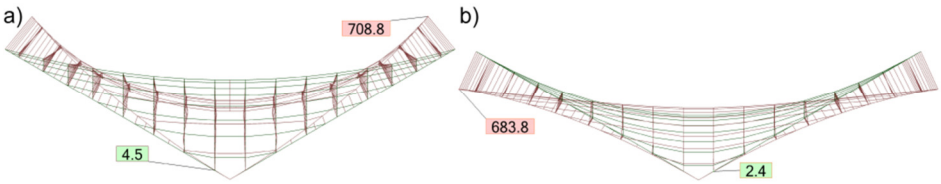

Fig. 11. Deformation of the structure for a) 1st and b) 2nd net shape (1.0P+1.0G+1.0S)

Table 2. Summary of internal forces and displacement values from net shaping analysis

Load case	No. of net shape	Number of pretensioned cables	Sag in the saddle point	Suspension cables		Edge beams			
				Mean tensile force	Max. vertical deflection	Max. compressive force	Max. in plane bending moment	Max. out of plane bending moment	Max. keystone displacement
			f_i	$N_{X,MEAN}$	$\Delta_{V,MAX}$	$N_{X,MAX}$	$M_{Y,MAX}$	$M_{Z,MAX}$	Δ_{MAX}
			[m]	[kN]	[mm]	[kN]	[kNm]	[kNm]	[mm]
Pretensioning forces 1.0P	**1.**	16	2.5	138.7	31.3	-1630.4	420.0	3846.9	-626.0
	2.	16	5.3	64.7	-113.9	-844.04	-1437.2	-1495.5	405.8
Load combination 1.0P+1.0G+1.0S	**1.**	16	2.5	313.2	534.2	-3718.1	3840.0	3082.7	-708.8
	2.	16	5.3	317.5	-119.4	-3685.2	616.0	-2475.8	683.8

3.4. Discussion

The results showed that suspension cables in the 1st net geometry required approximately twice as large pretensioning forces as the alternative concept in order to obtain comparable tensile forces under load combination. The same values of axial forces in these members under pretension case only were unable

to be achieved. This might be due to different net shaping, which induced diverse internal force distribution and global behaviour of the numerical model.

The analysis indicated proportional relationship between tensile forces in suspension cables and compressive forces in the edge beams in all cases. In contrast, the distribution and values of bending moments were varied. The pretension induced larger in plane bending moments in the 2nd concept, while the inclusion of gravity load caused the opposite trend. The largest difference was observed in case of load combination, where the maximum value in the 2st concept was 84% smaller comparing to the 1st variant. The diverse net shape resulted in opposite distribution of out-of-plane bending moments. Maximum values obtained with the 2nd net geometry were 20–61% smaller in relation to the 1st version. In general, the 2nd concept of net shape appeared to be more effective in terms of overall bending in the edge arches.

Significant impact of net shaping was observed in the deformation view of the structures. The 1st structure showed downward deflection of roof cables, followed by inward displacement of edge beams. In this case, potential implementation of cable stays would counteract the inward folding and provide balance as well as greater model stability. In contrast, the analysis indicated an undesired outward displacement of the edge beams and upward deflection of the cable net in the 2nd alternative. This form of deformation disqualified the 2nd concept in view of further implementation of pretensioned cable stays. On this basis, the 1st concept of net shape was selected for the main part of the study, in which the simulation of indirect pretensioning was performed.

4. Analysis of structures with indirect pretensioning

4.1. Adaptation of the structure

The structural model with the selected net shape was implemented with 12 cable stays with a diameter of 50 mm, fixed to the edge beams (Fig. 12.a). Different levels of anchor points were designed to provide integration into a slope of a potential grandstand. At this stage of analysis, both edge beams were simply supported (Fig. 12.b). This modification was necessary to perform indirect pretensioning of roof cables, which is caused by the outward rotation of arches. Balance of the structure was provided by the implemented stays, which became the only cable members subjected to shortening. The described adaptation of the system was inspired by the discussed cable-roof structure in Koszalin. This variant is introduced as the 1st concept of indirect pretensioning in the study. Views of the structural model representing this concept are shown in Fig. 13.

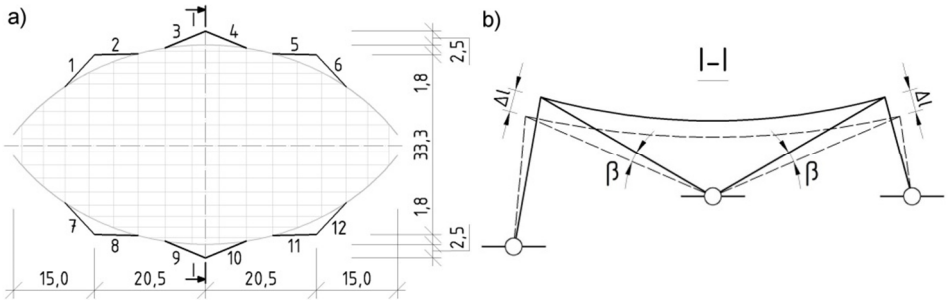

Fig. 12. Views of the structure showing a) the arrangement of cable stays in plan and b) simplified static scheme in cross section considering 1st concept of indirect pretensioning

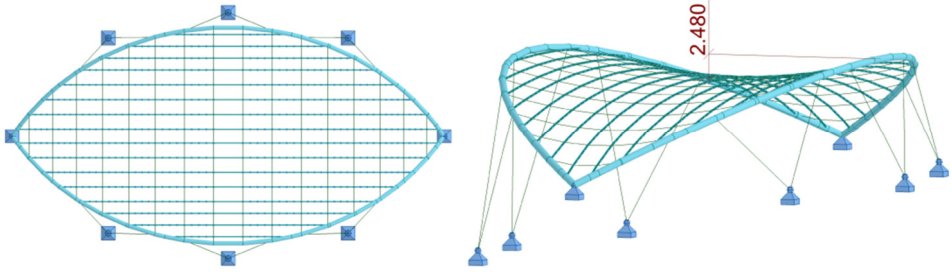

Fig. 13. Views of the structural model without roof panels representing the 1st concept of indirect pretensioning

The 2nd concept of indirect pretension assumed stiffening of the supporting structure and reducing the number of cable stays. The alternative version retained the arrangement of net shape and stays, whilst the supporting conditions were modified. The group of shorter cable stays no. 7–12 was replaced by CHS 159×10 members (Fig. 14.b). Furthermore, the stiffened edge beam received fixed supports (Fig. 14.a). In this case, the indirect pretension action was simulated by the limited group of 6 longer stays, fixed to the simply supported arch (Fig. 14.a).

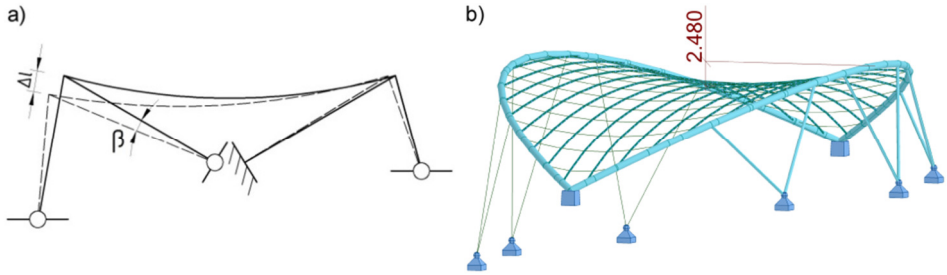

Fig. 14. 2nd concept of indirect pretensioning represented by a) simplified static scheme in cross section and b) view of structural model without roof panels

4.2. Assumptions of pretensioning

At this stage of the study, suspension cables were free of initial shortening in the software. This operation was performed on the implemented cable stays, where the values of relative dilatation were set on the same level in both versions. This parameter was adjusted in order to obtain comparable deflection of cables under load combination in reference to the results of the net shaping analysis. In this regard, the values of this parameter equaled:

- 0.008 in long and 0.012 in short stays in the 1st pretension concept,
- 0.008 in long stays in the 2nd pretension concept.

The prestress applied to the cable stays led to the outward rotation of the simply supported arches. The difference between the original and final position of the edge beams was described by the β angle of rotation and approximate to:

- 0.5° in the 1st pretensioning concept,
- 0.4° in the 2nd pretensioning concept.

4.3. Results

Several diagrams of internal forces and deformation for cable stays, suspension cables and edge beams, considering the 1st and 2nd concept of indirect pretension are presented in Fig. 15–20. The summary of internal forces and displacement values is given in Table 3.

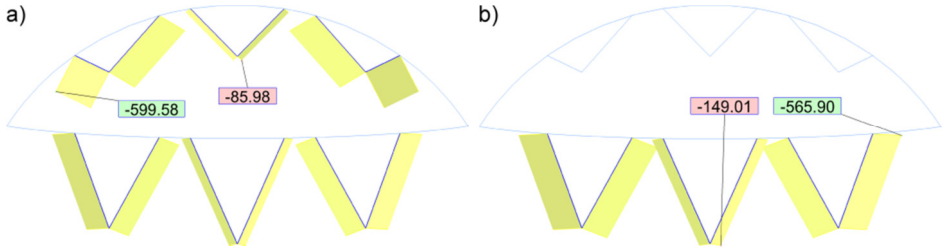

Fig. 15. Axial forces N_X in cable stays for a) 1st and b) 2nd pretensioning concept (1.0P)

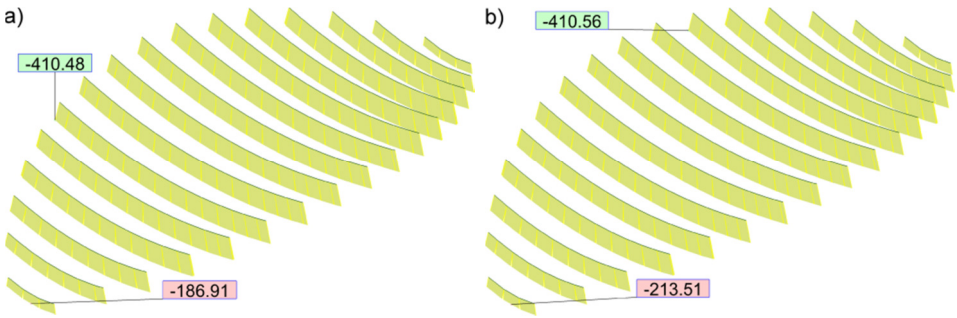

Fig. 16. Axial forces N_X in suspension cables for a) 1st and b) 2nd pretensioning concept (1.0P)

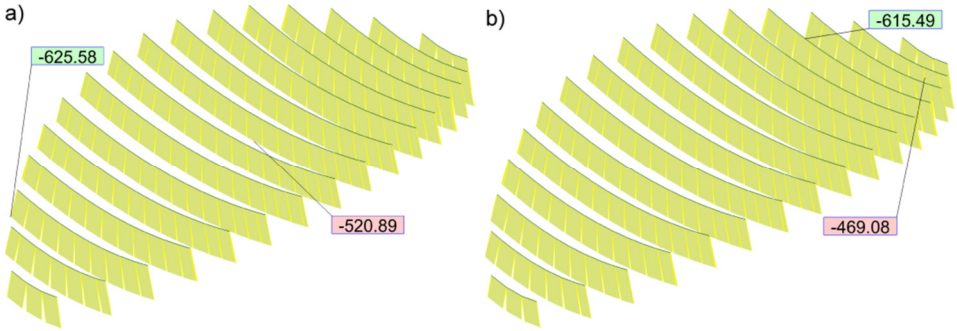

Fig. 17. Axial forces N_X in suspension cables for a) 1st and b) 2nd pretensioning concept (1.0P+1.0G+1.0S)

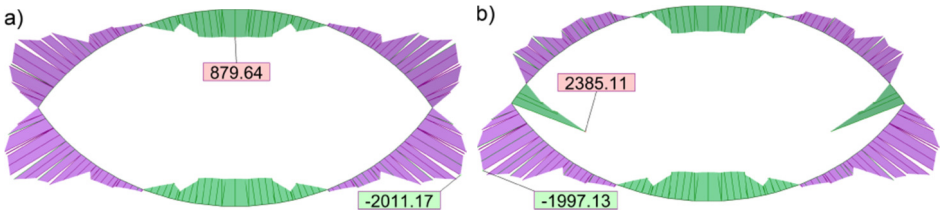

Fig. 18. In plane bending moments M_Y in edge beams for a) 1st and b) 2nd pretensioning concept (1.0P+1.0G+1.0S)

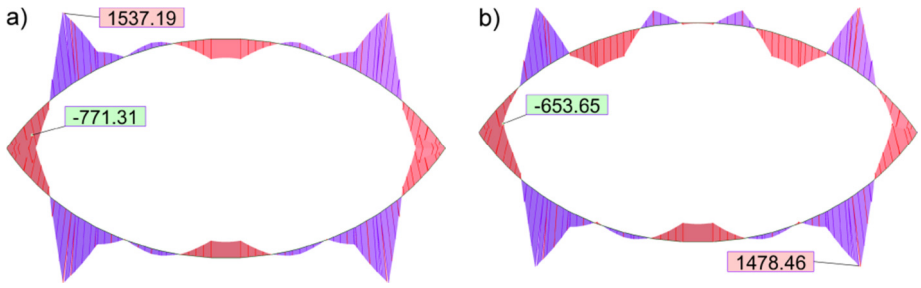

Fig. 19. Out of plane bending moments M_Z in edge beams for a) 1st and b) 2nd pretensioning concept (1.0P+1.0G+1.0S).

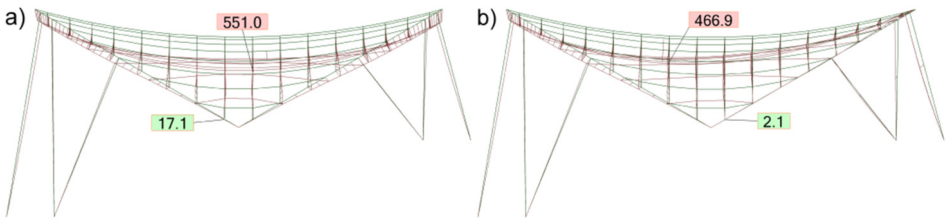

Fig. 20. Deformation of the structure for a) 1st and b) 2nd pretensioning concept (1.0P+1.0G+1.0S)

Table 3. Summary of internal forces and displacement values from indirect pretensioning analysis

Load case	No. of pretensioning concept	Number of pretensioned stays	Stays	Suspension cables		Edge beams			
			Max. tensile force	Mean tensile force	Max. vertical deflection	Max. compressive force	Max. in plane bending moment	Max. out of plane bending moment	Max. keystone displacement
			$N_{X,MAX}$	$N_{X,MEAN}$	$\Delta_{V,MAX}$	$N_{X,MAX}$	$M_{Y,MAX}$	$M_{Z,MAX}$	Δ_{MAX}
			[kN]	[kN]	[mm]	[kN]	[kNm]	[kNm]	[mm]
Pretensioning forces 1.0P	**1.**	12	599.6	379.5	-59.0	-4162.2	450.7	867.3	197.1
	2.	6	565.9	381.9	-132.3	-4155.2	465.2	-1134.8	166.7
Load combination 1.0P+1.0G+1.0S	**1.**	12	847.3	564.0	551.0	-5921.6	-2011.2	1537.2	202.3
	2.	6	753.6	565.4	466.9	-5820.8	2385.1	1478.5	175.4

4.4. Discussion

The results showed that despite the reduction of prestressed stays, the structure representing the 2nd concept responded with approximately equal axial forces in suspension cables comparing to the 1st solution. In both variants, these values showed a proportional relationship under introduced load cases. This trend may be considered similar regarding cable stays.

Compression of the edge beams was proportional to the tensile forces in cables and similar in both concepts. Minor differences appeared in the bending moment values due to the implementation of fixed supports in one of the edge beams in the 2nd pretension concept. Maximum difference was observed for the in-plane bending moment under characteristic load combination. In this case, the value in the 2nd concept was 20% greater in reference to the 1st variant. Apart from this, the analysis indicated comparable bending moment distribution along the arches span.

The deformation forms differed due to the applied pretensioning method. The 1st concept showed similar displacements in both arches, whilst the deformation view representing the alternative was slightly asymmetrical. This behaviour resulted from stiffening one of the edge beams, which retained its position under the applied load. However, the maximum values of displacement for each member occurred to be smaller in the 2nd variant. The application of this modified method caused a reduction of cable net deflection up to 15% in relation to the 1st concept.

5. Summary and conclusions

In this paper, the results of the finite element analysis of several cable net roof structures are presented. The concepts were investigated in the aspects of structural net shaping and application of different pretensioning methods. In this regard, the analysis was divided into two stages. Each part involved the numerical study of two concepts of the structure, which represented different solutions in terms of the analysed aspects. The favourable variant of net shape constituted the geometrical basis for the further analysis of various pretension concepts. The presented applications were inspired by the indirect pretension performed during the completion of cable net roof over the open-air theatre in Koszalin. All of the introduced solutions were assessed on the basis of comparison of the system response under pretension and the inclusion of gravity load.

The results of the net shaping analysis of the self-balanced systems proved that the geometry of cables has significant impact on the behavior of the structure. The surface with typical sag-to-span ratio was compared to the proposed curvature of cables aimed to reduce bending of edge beams. The variants showed diverse response under considered load cases. Significant reduction of bending in the arches for the alternative geometry was achieved. Nevertheless, this concept appeared to be unfavourable in terms of further application of indirect pretension. Large sag of the surface in addition to nonlinear behavior of cables induced outward displacement of the arches, which eliminated the implementation of prestressed cable stays in further steps. Moreover, the deformation form showed an atypical upward deflection of the cable net under gravity load, which might disqualify this geometry as the solution for self-balanced supporting structure. On these grounds, the concept with typical sag to span ratio was selected as a base model for simulations of indirect pretensioning in the main part of the study.

The application of indirect way of pretensioning in cable net numerical models proved to be effective for the inspired concept as well as the introduced alternative, in which a reduced number of prestressed cable stays was responsible for the pretensioning of the cable roof. The numerical implementation of these solutions induced the assumed pretension of the cable net in the introduced systems. The results showed approximately similar values of internal forces distribution in both concepts. Greater maximum bending moment values were observed in some cases due to the implementation of fixed support in one of the arches. The application of the proposed method, aimed to limit the number of cable stays, gained favour in terms of model stability. Stiffening of the supporting structure resulted in smaller values of displacement for roof cables and edge beams in comparison to the application of unmodified method inspired by the completion of the cable roof in Koszalin.

The numerical verification of consecutive concepts led to a gradual reduction of directly prestressed members from 16 suspension cables to 6 cable

stays in the analysed roof. The idea presented in the final proposal might be beneficial in terms of complexity and time of roof erection, which depends on the process of prestressing cable members. Moreover, successful implementation of indirect pretensioning eliminates the need to use tensioning devices at great heights. The proposed method of stiffening one of the edge beams might be favourable in the aspect of roof construction. The self-balanced arch can support the whole cable system during the erection of the structure. Nevertheless, the introduced solution shall be investigated under upward action of wind, which may indicate problems with balance of this type of system. Such application shall also be analysed in view of stiffness of joints and supports in the structure. A wider parametric analysis of the net shape might also be considered in order to obtain optimal cables geometry in view of the applied pretensioning method.

References

[1] Buchholdt, H. A. An introduction to cable roof structures, second edition, Thomas Telford, London, 1999.

[2] Pałkowski, S. Steel structures, Some issues of calculating and designing, Polish Scientific Publishers PWN, Warsaw, 2009 (in Polish).

[3] Łubiński, M.; Żółtowski, W. Metal structures, Part 2, Arkady, Warsaw, 2004 (in Polish).

[4] Pałkowski, S. Cable structures, Scientific-Technical Publishers WNT, Warsaw, 1994 (in Polish).

[5] Kucharczuk, W.; Labocha, S. Steel structure halls, Designers guide, Polish Technical Publishers PWT, Rzeszow, 2012 (in Polish).

[6] Jankowiak, W. Selected issues of steel structures, Part 2 – Tanks, Storage bins, Suspended structures, PUT Publishing House, Poznan, 1994 (in Polish).

[7] Filipkowski, J.; Deska, K. Geometrical framework of a suspended structure and the state of displacement due to snow load, 25th International Conference on Structural Failures, Międzyzdroje, May 2011 (in Polish).

[8] Bradshaw, R. History of the analysis of cable net structures, Proceedings of the 2005 Structures Congress and 2005 Forensic Engineering Symposium, New York, April 2005.

[9] Pawłowski, W.; Deska, K. Registration of geometrical structure of suspended roof for example of the open-air theatre roof in Koszalin, Scientific Bulletin of Lodz Technical University: Civil Engineering, v. 60, no. 1052, Lodz University of Technology Press, Lodz, 2009, 97–105 (in Polish).

[10] PN-EN 1991-1-3: 2005 Eurocode 1: Actions on structures – Part 1-3: General actions – Snow loads (in Polish).

[11] EN 1993-1-11: 2006 Eurocode 3: Design of steel structures – Part 1-11: Design of structures with tension components.

Przesłano do redakcji: 09.12.2019 r.

CZASOPISMO INŻYNIERII LĄDOWEJ, ŚRODOWISKA I ARCHITEKTURY
JOURNAL OF CIVIL ENGINEERING, ENVIRONMENT AND ARCHITECTURE
JCEEA, t. XXXVI, z. 66 (3/19), lipiec-wrzesień 2019, s. 65-76, DOI:10.7862/rb.2019.18

Maciej PIEKARSKI[1]

RENEWAL OF SELECTED FRAGMENTS OF RZESZÓW BASED ON THE LOST SYMBOLS AND FUNCTIONS OF PLACES AS A MEANS OF STRENGTHENING THE CITY'S IDENTITY

The article discusses the method of revitalizing public space, consisting of recreating local stories, after which no artefacts have survived, and telling them to pedestrians by means of innovative interactive objects of small architecture and urban furniture. The method is based on literature research, as well as observation and descriptive analysis of the surrounding landscape. Development plans for two fragments of the center of Rzeszów are described in detail: the crossing of Grunwaldzka and Bernardyńska streets and the part of Mickiewicz street. In the first location, the sculpture presenting life-size figure of photographer Edward Janusz, whose atelier functioned near-by at the turn of the 19th and 20th century, is planned to be placed. One of the elements of the sculpture is to be an old-fashioned camera with a digital camera inside, which will take photos of interested persons, and insert the contemporary photo into the photo taken from this place by Edward Janusz. The reference to cultural heritage in the Mickiewicz street restoration project comes down to recalling non-existent buildings in an augmented reality environment, as well as to reminding Two Pump Square, a former meeting place for residents coming for water. The function of former water pumps will be realised with the use of two bicycle wheel pumps and movable seats will be located in the vicinity.

Keywords: public space, city's identity, cultural heritage, innovations

1. Introduction

Rzeszów is a city that has transformed during the last 80 years from a small town into a 200,000-strong city. Now, population growth is caused by settlement of young people who after completing education in Rzeszów find in it a friendly haven for their further life stage. The population growth is accompanied by the city's spatial expansion. Rzeszów's quantitative success coincides with development of entities whose activity bases on the high technology industry.

[1] Maciej Piekarski, Rzeszow University of Technology, Faculty of Civil and Environmental Engineering and Architecture, Department of Architectural Design and Engineering Graphics, al. Powstańców Warszawy 12, 35-959 Rzeszów, Poland, tel. +48 17 8651839, e-mail: mgpiekar@prz.edu.pl, ORCID: 0000-0002-9788-1099

The city's advertising slogan is: *Rzeszów - the Capital of Innovation*. Such an image brand does not fully express the city's identity, because it does not refer at all to its heritage, which although is not clearly visible in such the transformed city, but finding it is not impossible. The author is searching for the ways of strengthening the identity of Rzeszów by reorganizing public space, which would expose better the city's cultural heritage shaping awareness about him in its new inhabitants. The achievement of this goal is proposed by enriching the public space with innovative objects that would universalize the memory of the heritage in a way adequate to the chosen image brand of Rzeszów. The idea of the concept is an evocation to realize in selected fragments of the historical city centre of three areas of time: the presence of past things, the presence of present things and the presence of future things [2]. The author believes that making within the historic centre of Rzeszów the public space more attractive will have a positive impact on the intensity of its exploration, and bringing the residents closer together and focusing their attention on the city's identity indicators will strengthen the sense of belonging to the local community.

2. Well organized public space and heritage as key factors creating identity of the city and its inhabitants

The word identity refers to continuing and remaining the same, as well as being separate and distinct [4]. The identity of the city is considered by the identity of its inhabitants, i.e. their individual sense of personal relationship with the city, as well as a set of those features of public space that stand out with unprecedented specificity. There is a close relationship between the identity of the spatial structure and the identities of its users. Cities last longer than people. The identity of old cities is due to their history. It is visible in the spatial arrangement and through preserved architectural objects. In relation to events whose material traces have been blurred, it remains in memory passed down from generation to generation. This condition is disturbed if the city is experiencing dynamic development, which is usually accompanied by a significant influx of people from outside. Mental identification of settlers with the city requires making an effort. The city authorities and local leaders, whose degree of identification with the city and motivation to act on its behalf are very high, should take on this challenge. The city's identity, which is the basis for the integration of newcomers, should refer to its history, but also take into account the circumstances that have become the reason for the sudden dynamic development of the city.

The quality of public space is presented as an important factor influencing the attitudes of residents in modern urban planning. Well-organized public space encourages people to stay in it for periods of time longer than just to meet the necessary needs, while being together with unknown people builds a sense of community. Fragments of public space that are organized as eye-catching

microcosms of meanings play a special role for the identity of cities. In the literature they are called places [15].

Place cannot be anywhere. The potential contained in the landscape, expressed through its physical features and imaginary contents emanating from them, is necessary. It is such a set of properties characterizing a specific section of space, which is referred to as *genius loci* [13]. Subsequently, the creation of the place is decided by a conscious choice called heritage, consisting in the intention to consolidate and pass on to posterity those testimonies of the past that respond to current demand and it is possible to applicate them in contemporary use [1]. Thanks to the designer's perceptiveness and creativity, they can be perpetuated in forms that tell about the past, present and future of the place [9]. So that the city could be read like a book [8].

The most attractive places where poetry and symbolism are combined with good organization of public space are becoming effective landmarks for the city's users. Their presence is necessary for the possibility of full assimilation of the city and identification with it [11]. Because attractive places entice people whose activity entices even more people to these places [6], attractive public spaces in city centres not only counteract the economic degradation of downtown caused by the outflow of permanent residents, but even contribute to their economic growth [16].

An important problem facing the designer of any public space, including one that due to the presence of genius loci in it aspires to the rank of place, is a good design of seating places. Benches that are most often chosen by pedestrians are those that provide a view of events in the environment, and especially allow observation of other people. A well-equipped public space should offer various seating options to create opportunities for different, larger and smaller groups of users to stay in it, as well as for individuals [5]. If there are many eye-catching landscape features in the environment, the placement of the benches should allow to choose to observe any of them. The last issue is the arrangement of the benches so that it allows you to choose not only sitting back to back or face to face, but also to place people in relation to each other in intermediate positions, which are more conducive to establishing communication [14].

3. The goal and methodology of the research

The research conducted has been focused on a problem specific for Rzeszów, but the applied methodology can be adopted in any localisation. The generalized goal of the study can be described as the transformation of selected fragments of the city, characterized by high landscape and historical potential, from places imperceptible into centres of emanating genius loci, which would attract people.

In the author's opinion, the main reasons for the fact that certain places are not expressive in the city's fabric, despite trumps in the form of a rich history

and preserved architectural objects remembering it, are disorder traffic and the lack of the objects or institutions able to generate high activity of residents. Permitting car traffic means that car users do not focus their attention on the landscape. First of all, traveling by car they are surrounded by a private space, that means the car's interior, which weakens the perception of the outside world [10]. Secondly, the attention of drivers is focused on analyzing the movement of other vehicles or searching for a place to park as close as possible to the destination. The attention of pedestrians and cyclists moving in such conditions, in turn, focuses on avoiding collisions with passing or parked cars. Therefore, the first point of the research work is to outline the boundaries of space that should be intended only for pedestrians, along with recommendations regarding the diversion of existing car traffic.

In the research issue aimed at the qualitative transformation of specific fragments of urban fabric, it is difficult to apply quantitative and statistical research methods. The study must be based on the method of logical argumentation, i.e. on analysis and logical construction. Useful research techniques are literature studies covering historical sources, people's memories and archival photographs and maps, as well as participatory observations and descriptive analyses [12]. With their help, you can visually reconstitute the nature of original human activity in a given area and determine the points from which the perception of the most valuable landscape elements is the best.

The next stage of the research boils down to the precise route tracing so as to force pedestrians to observe what is most valuable, and to arouse interest in their past by enriching public space with objects referring to the former functions of places. Making the space available to pedestrians is the basic generator of activity. A side effect is a change in the speed of the movement. The space travelled on foot is penetrated by the eyesight much more accurately than the space travelled by car or at least by bicycle [6]. Creation a crossing point of routes in a transformed place is very valuable. The location of additional activity generators, e.g. in the form of atypical small architecture objects, including seating furniture, will contribute to the creation of a real nodal place, whose surroundings will attract the activities of entities offering services previously absent in this location.

4. Cases studies

4.1. Grunwaldzka street

Grunwaldzka Street was in the past a communication route leading traffic towards Sandomierz. Currently, its section between Kościuszko and Sobieski Streets (Fig. 1) serves as a promenade. The crucial point on this section is the intersection with Bernardyńska Street in the form of a small square. The closing of the perspective of Bernardyńska Street visible from this place is the silhouette

Fig. 1. The fragment of Rzeszów with places considered in the article

of the 17th century church of the Bernardine's. This landscape value is not exposed, because the section of the street adjacent to Grunwaldzka Street is actually a half-official - half-wild parking lot. Pedestrian traffic along Bernardyńska Street practically does not exist, because it is discouraged by narrow pavements and the lack of service offer that would generate this traffic.

Near the street intersection, in the building at Grunwaldzka 18, Edward Janusz (Fig. 2a) opened in 1886 a photo studio [7]. Thanks to his extraordinary talent, he quickly gained the reputation of an excellent portraitist. Having the photo taken by Janusz became the ambition of the inhabitants of Rzeszów and the surrounding area. The fame of the atelier (Fig. 2b), which was to 1968 managed by the founder's family, outlasted after the death of Edward Janusz in 1914. The studio was finally closed in the 1990s. In 1997, the legend of Edward Janusz was revived again. In the attic of the house where the atelier was located, 30,000 glass negatives were preserved in perfect condition. They are a unique resource of the cultural heritage of Rzeszów. The idea of reviving this place at the intersection of the streets is based on the legend of Edward Janusz and the photo he took, which shows a view from this square towards the Bernardine church.

a) b)

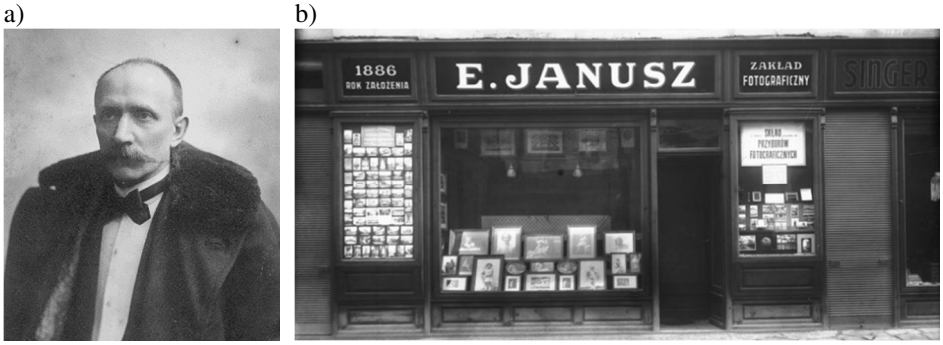

Fig. 2. a) Edward Janusz, b) Edward Janusz's photo studio

Fig. 3. The concept and localization of sculpture of Edward Janusz with his old-fashioned camera equipped with a modern digital camera inside

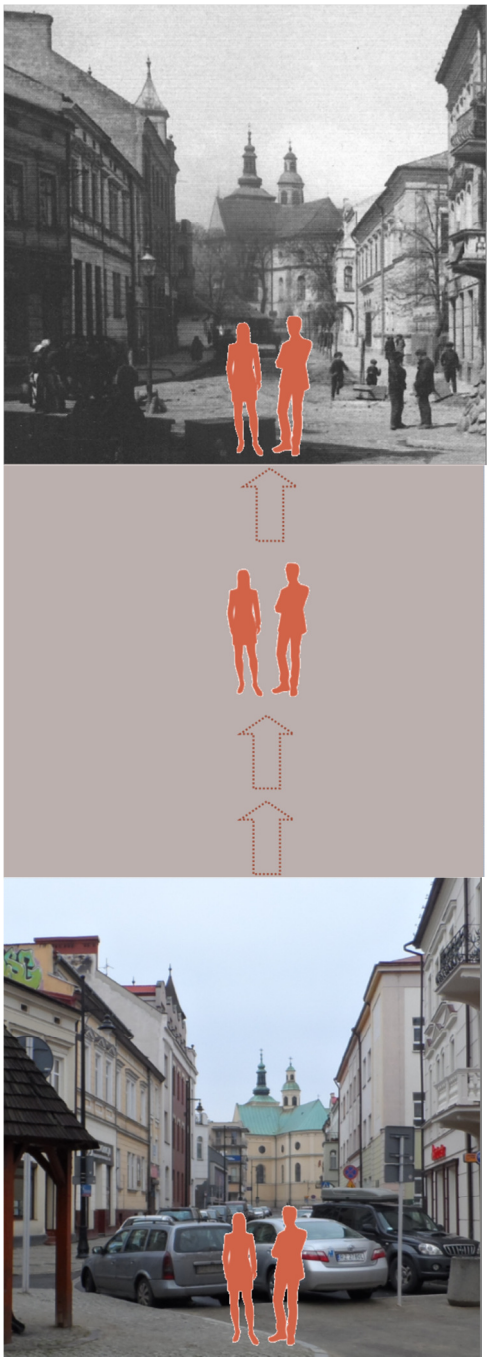

Fig. 4. The concept of making photos referring to the historical appearance of the place, with the use of the camera installed in the monument of Edward Janusz

The author's concept includes placing a sculpture at the crossing of Grunwaldzka and Bernardyńska Streets, showing the life-size figure of Edward Janusz, who is taking a photo with an old-fashioned camera placed on a tripod (Fig. 3). The model of the nineteenth-century camera will be equipped with a digital camera, photographing willing people using a dedicated smartphone application. The original photo taken by Edward Janusz is planned to be used as the background on which the photographed persons will be presented. The project also involves placing next to movable benches, which would allow changing the observed view in accordance with preferences of resting people, as well as switching off car traffic on the dead end of Bernardyńska Street. After the revitalization of this place, residents of Rzeszów and visiting the city, just like they used to, will be able to "go to Janusz" to take a picture, and also observe the "work" of a 19th century photographer (Fig. 4).

4.2. Mickiewicz street

Mickiewicz Street connects the Market Square with Targowa Street (Fig. 4). It is one of the oldest streets in Rzeszów. It used to be an exit road to the east. For almost 120 years, residents were also undergoing their last trip this road. At the end of the street there is the Old Cemetery with the classical chapel of St. Trinity. In the middle part the street was once narrower than today. The buildings marking the southern side of the street were standing in the place of the nowadays strip separating roadways and they formed the spaces of two piazzas non-existing today. On both piazzas there were pumps, which through the utility function integrated the community of nearby houses [3]. The buildings were demolished during the German occupation in the period of World War II. The tightly built-in place was replaced by an open space in which two street roadways were marked out. The loss was compensated by the unveiling of the viewing axis marked out by the bell tower of the parish church and the monument of Adam Mickiewicz. Unfortunately, the axis is located on the southern roadway, where traffic is allowed. In turn, allowing traffic and parking cars on the northern road deprives pedestrians of the possibility of perceiving the chapel of St. Trinity. The qualities of the street are aggravated by the presence of a public toilet, while they are strengthened by the vicinity of the successfully arranged space of Cichociemni Square, with the sculpture of Józef Szajna "Passage".

In response to the announcement made by the mayor of Rzeszów of the intention to revitalize Mickiewicz street combined with the elimination of car traffic, the author prepared a concept for developing a section of this street between the crossings with Joselewicz and Gałęzowski streets. The project includes the following elements:

- directing pedestrian and cyclist traffic,
- restoring the memory of former buildings by marking the place occupied by buildings in the street pavement and recreating their solids in an augmented reality environment,

- reminder about Two Pumps Square by installing stationary bicycle pumps,
- reactivation of the integrating street function by organizing a place creating a "city salon", equipped with sets of rotating benches whose orientation in space can be adjusted for the needs of meetings in larger or smaller groups, or the organization of the audience for events taking place on one side.

The condition of canalizing the traffic of pedestrians and cyclists is to eliminate car traffic. The demarcation of a pedestrian promenade is envisaged on the southern side of the northern roadway, while the southern roadway is to be converted into a pedestrian street along with the location within it of a set of seats forming the so-called city lounge. Cyclists will have the separated space between areas once occupied in the past by buildings (Fig. 5).

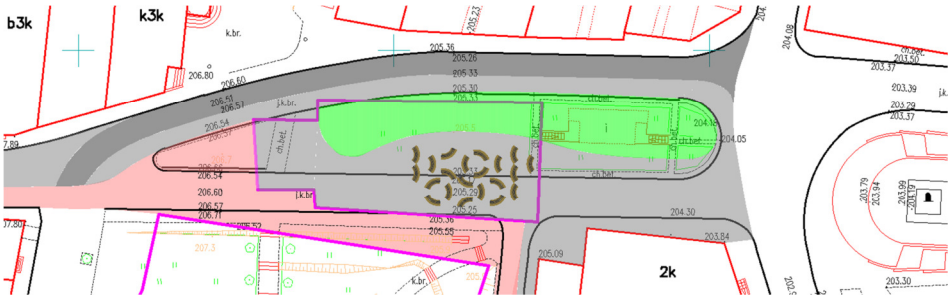

Fig. 5. The concept of organization of the space within Mickiewicz street

Fig. 6. The perspective of Mickiewicz street: a) historical view, b) nowadays view with marked the solid of non-existing building

The starting point for the presentation of former buildings in augmented reality technology is to build a digital model made on the basis of preserved maps, drawings and photographs. Access to the model is assumed using stereoscopic stationary devices, which also would emit a signal allowing for omni-directional view of objects with the use of a smartphone and a special application. The intention is not to present buildings with photographic

accuracy, but to show contour ghost-houses superimposed on the image of the real environment (Fig. 6).

The basic procedure to restore the memory of Square of Two Pumps (Fig. 7a) will be the installation of two bicycle pumps, one of which could refer to a traditional tire pump in the form (Fig. 7b), the other – to a street well (Fig. 7c). The location of pumps and more bicycle racks in their vicinity, together with the presence of a nearby city salon, will restore the former social function, orienting it towards the integration of the cyclist's community.

The location of the municipal salon is planned in a place previously occupied by demolished buildings, from which it is possible to perceive the three dominants: the Mickiewicz monument (Fig. 8a), the sculpture "Passage" (Fig. 8b) and the parish belfry (Fig. 8c). The living room is to reflect the idea of a house in which residents - inhabitants of Rzeszów can feel at ease, which will be confirmed by the possibility of free turning the seats in installed benches. It is anticipated that the benches will be combined into three-piece modules, in which the rotation of the seats will be interdependent, as a result of joining them by means of mechanisms hidden under the surface of the promenade (Fig. 9). The double symbolism characterize the correlation of bench rotations: inhabit-ants of a shared house do not operate on their own, and the future, although unknown and multiple, is determined by the existed circumstances. The configuration of the benches in addition to expressing this symbolism, meets the needs of people coming in groups or individually, wanting to maintain a minimum of intimacy in the public space or seeking integration with other people, as well as having different preferences in perceiving architectural landscape views. The multitude of seats means that everyone will be able to use this space according to their preferences.

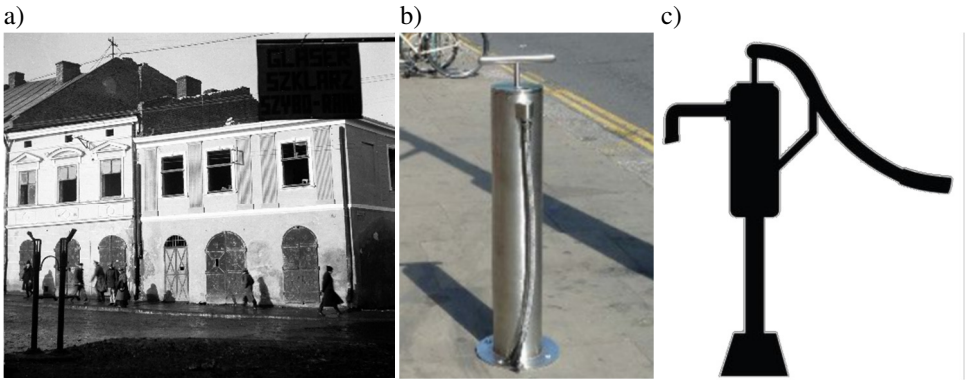

Fig. 7. Two Pumps Square: a) historical photo, b, c) ideas of the pumps for bike tires

Fig. 8. The dominants visible from Mickiewicz street: a) the Mickiewicz monument, b) the sculpture "Passage", c) the parish belfry

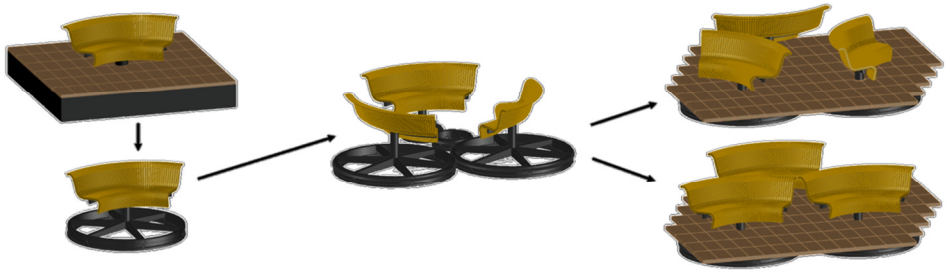

Fig. 9. The concept of rotary benches

5. Conclusion

In the author's opinion, the key achievement of the presented methodology of revitalizing public space is to reconstruct local stories after which no artefacts have survived and to tell it with the help of modern devices to pedestrians traversing the city space. The effectiveness of the method is first difficult to assess at the stage preceding the actual implementation in public space, and secondly, it depends to a large extent on the inventiveness of the researcher - the designer of public space development, as well as the artistry of the designer of small architecture objects. The evaluation of a project implemented in real terms can be made by collecting the opinions of city residents, and in the most objective way, by measuring the change in pedestrian traffic in the area.

The article presents ideas of spatial changes in two parts of the strict centre of Rzeszów, whose potential is not fully exploited. They can be treated as a part of a wider district revitalization plan, which due to the limited volume of the article has not been presented in it. It is also possible to tell other stories using appropriately selected means. The author believes that the use of unusual, unparalleled functional solutions in elements of small architecture and urban furniture will influence into an increase in interest in the part of the city where huge heritage capital is contained.

References

[1] Ashworth G.: Planowanie dziedzictwa, Międzynarodowe Centrum Kultury, Kraków 2015.

[2] Augustyn: Wyznania, Znak, Kraków 2018.

[3] Czarnota M.: Rzeszowskie ulice i okolice, Mitel, Rzeszów 2011.

[4] Dymnicka M.: Tożsamości miejskie [w: Bierwiaczonek K, Dymnicka M., Kajdanek K., Nawrocki T.: Miasto, przestrzeń, tożsamość – studium trzech miast Gdańsk, Gliwice, Wrocław}, Scholar, Warszawa 2017.

[5] Gehl. J.: Życie między budynkami. Użytkowanie przestrzeni publicznych, Wydawnictwo RAM, Kraków 2013.

[6] Gehl J.: Miasta dla ludzi, Wydawnictwo RAM, Kraków 2014.

[7] Kaliszewska E., Krzysztofowicz K.: Czas w kadrze zatrzymany. Edward Janusz i jego fotografie, Fundacja Rzeszowska, Rzeszów 2018.

[8] Kłosek-Kozłowska D. 2017. Ochrona wartości kulturowych miast a urbanistyka. Warszawa: Oficyna Wydawnicza Politechniki Warszawskiej.

[9] Królikowski J. T.: Projektowanie krajobrazu miasta zaczyna się od rozpoznania znaczeń i wartości [w: Projektowanie krajobrazu miasta (red. J. T. Królikowski, K. Rybak-Niedziółka, E. A. Rykała)], Wydawnictwo SGGW, Warszawa 2017.

[10] Lofland L. H. A World of Strangers. Order and Action in Urban Public Space, Basic Books, New York 1973.

[11] Lynch K.: Obraz miasta, Wydawnictwo Archivolta Michał Stępień, Kraków 2011.

[12] Niezabitowska E.: Metody I techniki badawcze w architekturze, Wydawnictwo Politechniki Śląskiej, Gliwice 2014.

[13] Norberg-Schulz Ch.: Genius loci. Towards a phenomenology of architecture, Rizzoli, New York 1980.

[14] Skibińska M.: Mebel miejski i wzornictwo [w: Projektowanie krajobrazu miasta (red. J. T. Królikowski, K. Rybak-Niedziółka, E. A. Rykała)], Wydawnictwo SGGW, Warszawa 2017.

[15] Tuan Y.F.: Przestrzeń i miejsce, Państwowy Instytut Wydawniczy, Warszawa 1987.

[16] Zuziak Z.: Strategie rewitalizacji przestrzeni śródmiejskiej, Politechnika Krakowska im. T. Kościuszki, Kraków 1998.

Przesłano do redakcji: 09.12.2019 r.

Additional information

1. The Journal annually publishes a list of reviewers: in the last issue of the quarterly - vol. 65 (4/18) and on the website:
   www.oficyna.prz.edu.pl/pl/zeszyty-naukowe/czasopismo-inzynierii-ladowej-s/
2. The journal uses as described on its website the procedure for reviewing:
   www.oficyna.prz.edu.pl/zasady-recenzowania/
3. Information for authors available at:
   www. oficyna.prz.edu.pl/informacje-dla-autorów/
4. Review's form available at:
   www.oficyna.prz.edu.pl/pl/zeszyty-naukowe/czasopismo-inzynierii-ladowej-s/
5. Instruction for Authors, which describes in detail the structure of the article, its layout, the way of preparing illustrative material and the literature is published on the website:
   www.oficyna.prz.edu.pl/pl/instrukcja-dla-autorów/
   and
   www.oficyna.prz.edu.pl/pl/zeszyty-naukowe/czasopismo-inzynierii-ladowej-s/
6. Contact details to Editorial Office, postal and e-mail addresses for sending articles and contact details to the publisher are provided on the website:
   www.oficyna.prz.edu.pl/pl/zeszyty-naukowe/czasopismo-inzynierii-ladowej-s/

Reviewing standards, information for authors, the review form, instruction for authors and contact details to JCEEA Editors and to Publishing House are also published in the fourth number of JCEEA vol. 66 (4/19).